Keeping an eye out for change: Anxiety disrupts adaptive resolution of policy and epistemic uncertainty

Amrita Lamba[1,3], Michael J. Frank[1,2], Oriel FeldmanHall[1,2]

Affiliations: [1]Department of Cognitive & Psychological Sciences, Brown University, Providence, RI. [2]Carney Institute of Brain Sciences, Brown University, Providence, RI. [3]Department of Brain & Cognitive Sciences, Massachusetts Institute of Technology, Cambridge, MA.

Abstract: Human learning unfolds under uncertainty. Uncertainty is heterogeneous with different forms exerting distinct influences on learning. While one can be uncertain about what to do to maximize rewarding outcomes, known as policy uncertainty, one can also be uncertain about general world knowledge, known as epistemic uncertainty. In complex and naturalistic environments such as the social world, adaptive learning may hinge on striking a balance between attending to and resolving each type of uncertainty. Prior work illustrates that people with anxiety—those with increased threat and uncertainty sensitivity—learn less from aversive outcomes, particularly as outcomes become more uncertain. How does a learner adaptively trade-off between attending to these distinct sources of uncertainty to successfully learn about their social environment? We developed a novel eye-tracking method to capture highly granular estimates of policy and epistemic uncertainty based on gaze patterns and pupil diameter (a physiological estimate of arousal). These empirically derived uncertainty measures reveal that humans flexibly switch between resolving policy and epistemic uncertainty to adaptively learn about which individuals can be trusted and which should be avoided. Those with increased anxiety, however, do not flexibly switch between resolving policy and epistemic uncertainty, and instead prioritize reducing epistemic uncertainty at the cost of optimizing behavior, leading to maladaptive behaviors with untrustworthy people.

Humans live and thrive in highly social environments (Buss, 1996; Ishii-Kuntz, 1990), despite encountering a great degree of uncertainty when interacting with others (FeldmanHall & Shenhav, 2019). This suggests that socially adaptive functioning requires individuals to efficiently resolve a multitude of uncertainty signals that can arise during a social exchange (Berg et al., 1995; Diaconescu et al., 2014; Fehr et al., 2005; FeldmanHall & Nassar, 2021; Kramer & Wei, 2014). Imagine, for instance, trying to figure out whether a new colleague can be trusted. In such scenarios, one may focus on reducing *policy uncertainty* (Franklin & Frank, 2015)—figuring out which set of actions produce desirable outcomes (i.e., *what should I do*?). For example, should I trust a colleague with sensitive information? If my colleague keeps a secret, then do I trust her again in the future? One can also focus on resolving *epistemic uncertainty* (Parr & Friston, 2017; Payzan-LeNestour & Bossaerts, 2011)—acquiring detailed knowledge and information about others. For example, you may closely observe your colleague's behavior to try to figure out exactly how trustworthy she is and what kinds of secrets she can keep (i.e., what are the precise outcomes I can *expect* from my actions?). While this type of value-based knowledge can increase the precision of one's beliefs allowing a learner to make more informed choices (Payzan-LeNestour & Bossaerts, 2011; Tomov et al., 2020), acquiring detailed epistemic knowledge is cognitively taxing (Parr & Friston, 2017; Wilson et al., 2021) and may not always offer additional benefit for optimizing rewarding outcomes (Friston et al., 2017).

While efficiently resolving each uncertainty signal provides distinct advantages for learning, overreliance on one signal at the expense of another can potentially result in maladaptive behavior. If we focus too much on minimizing policy uncertainty, our behavior might become too rigid, and we may not learn sufficient information that would allow us to generalize across contexts (Jaskir & Frank, 2023; Palminteri et al., 2015). If we focus too much on reducing epistemic uncertainty, we might end up investing too many resources gathering irrelevant information, which can ultimately slow learning (Parr & Friston, 2017; Wilson et al., 2021). While it appears that people are able to strike a delicate balance between optimizing rewarding outcomes and gathering additional knowledge when the opportunity arises, it is unknown how humans effectively manage such tradeoffs to facilitate adaptive learning.

Reinforcement Learning (RL) frameworks elegantly illustrate this learning dichotomy. While value-based (e.g., Q-learning) models iteratively learn the expected values of each action (Daw, 2011; Niv et al., 2006; Sutton & Barto, 2018)—a form of epistemic knowledge, policy-based models (e.g., actor-critic) directly optimize choice policies that maximize rewards without explicitly learning the expected values (Bennett et al., 2021; Collins & Frank, 2014; Li & Daw, 2011; Littman, 1994; Sutton & Barto, 2018). Although both strategies facilitate learning, it is often more expedient to directly optimize a policy by identifying the best set of actions, given that value-based methods exhibit slowed convergence to expected values and these misestimation errors impede performance (Jaskir & Frank, 2023; Mnih et al., 2015). And yet, solely relying on policy optimization can prevent people from gathering value-based information which can be useful if one needs to transfer knowledge to a novel problem (Jaskir & Frank, 2023; Palminteri et al., 2015). Thus, despite the efficiency of policy-optimization, humans should also assign utility to epistemic knowledge (Cohen et al., 2007; Friston et al., 2017; Schulz & Gershman, 2019; Wilson et al., 2014)—especially in the social world where epistemic information can help learners distinguish between the value of others (FeldmanHall & Nassar, 2021; Vives & FeldmanHall, 2018). This tradeoff suggests that adaptive human behavior may actually emerge from a combination of policy

optimization and value-based learning strategies (Collins & Shenhav, 2022; Niv & Langdon, 2016). Yet, how these strategies are combined to guide learning remains largely unknown (Nachum et al., 2017). One way to effectively manage this inherent tension is by dynamically orienting attention towards value or policy-based information as new task demands arise (Gottlieb et al., 2014), such that information sampling patterns might unveil how distinct uncertainty signals are prioritized for learning (Gottlieb et al., 2013; Gottlieb & Oudeyer, 2018).

In the current study we test the hypothesis that adaptive social learning is characterized by flexible and frequent attention switching between policy and epistemic information to regulate learning rates. Specifically, we evaluate whether people first reduce policy uncertainty to improve task performance, and then flexibly switch to gathering value-based information to further minimize epistemic uncertainty. This requires tracking subjective experiences of policy and epistemic uncertainty in real time as people manage these competing demands. Prior work suggests that eye movement provides a reliable readout of uncertainty (Bakst & McGuire, 2021; Leckey et al., 2020), revealing *what* information is being attended to—i.e., expected values or information related to the choice policy (Harris et al., 2023; Wittek et al., 2016). Moreover, using gaze patterns to measure uncertainty offers the advantage of sidestepping issues with existing measures (Garland, 1991; Subedi, 2016) that constrain the granularity of subjective uncertainty estimates to a single point estimate (Likert scales), and thereby omit critical details about the degree and type of uncertainty experienced. Given that fluctuations in uncertainty are also accompanied by increased physiological arousal (Bechara et al., 1996; Critchley et al., 2001; FeldmanHall et al., 2016), we can further index pupil-based arousal to the rate of learning adjustment (Aston-Jones & Cohen, 2005; Browning et al., 2015; Nassar et al., 2012; Urai et al., 2017), to test for the first time whether this system distinguishes between value-based epistemic uncertainty and policy uncertainty.

Finally, we also explore whether increased uncertainty sensitivity disrupts one's ability to leverage policy and epistemic uncertainty to effectively guide learning. It is well known that individuals with increased trait anxiety experience increased distress and intolerance towards uncertainty (Bishop, 2007; Boelen & Reijntjes, 2009; Buhr & Dugas, 2009; Carleton et al., 2012; Koerner & Dugas, 2006), and this hypersensitivity impacts one's ability to swiftly adjust behavior in uncertain environments (Aylward et al., 2019; Browning et al., 2015; Gagne et al., 2020; Lamba et al., 2020). Although prior work hints that anxious individuals fail to expediently adjust their behavior when policy uncertainty increases (Lamba et al., 2020), altered learning could potentially emerge because anxious individuals invest disproportionate cognitive resources gathering social knowledge. Given that the coupling between uncertainty and physiological arousal is blunted in people with increased anxiety (Browning et al., 2015), we can additionally leverage gaze patterns and pupillometry to directly test whether failures in tracking policy *or* epistemic uncertainty impinge on learning.

In the current research we construct empirically-derived estimates of policy and epistemic uncertainty from eye gaze, allowing us to examine how individuals direct their attention towards policy and epistemic uncertainty signals as social interactions unfold. To dissociate between policy and epistemic uncertainty, we implement a novel eye-tracking procedure in which participants indicate trial-level predictions about another's trustworthiness using their eye gaze. We find that task performance is predicted by how quickly an individual first resolves policy uncertainty and is

then able to flexibly switch to resolving residual value-based epistemic uncertainty. Adaptive switching is yoked to how much a partner's behavior changes during the task (i.e., becoming increasingly untrustworthy) and is reflected in pupil-based arousal. However, the behavioral and physiological fingerprint of flexibly switching between resolving different types of uncertainties is altered in highly anxious individuals. We fit a Bayesian RL model which further reveals that people with increased anxiety are slower to adjust their behavior as partners become increasingly untrustworthy because of a tendency to perseverate on prior reward history, even when learned values no longer reflect the statistics of the environment. This slowed learning is linked to an asymmetric focus on gathering social knowledge about partners, rather than optimizing one's choice policy, providing a novel mechanistic understanding of the learning objective of anxious individuals.

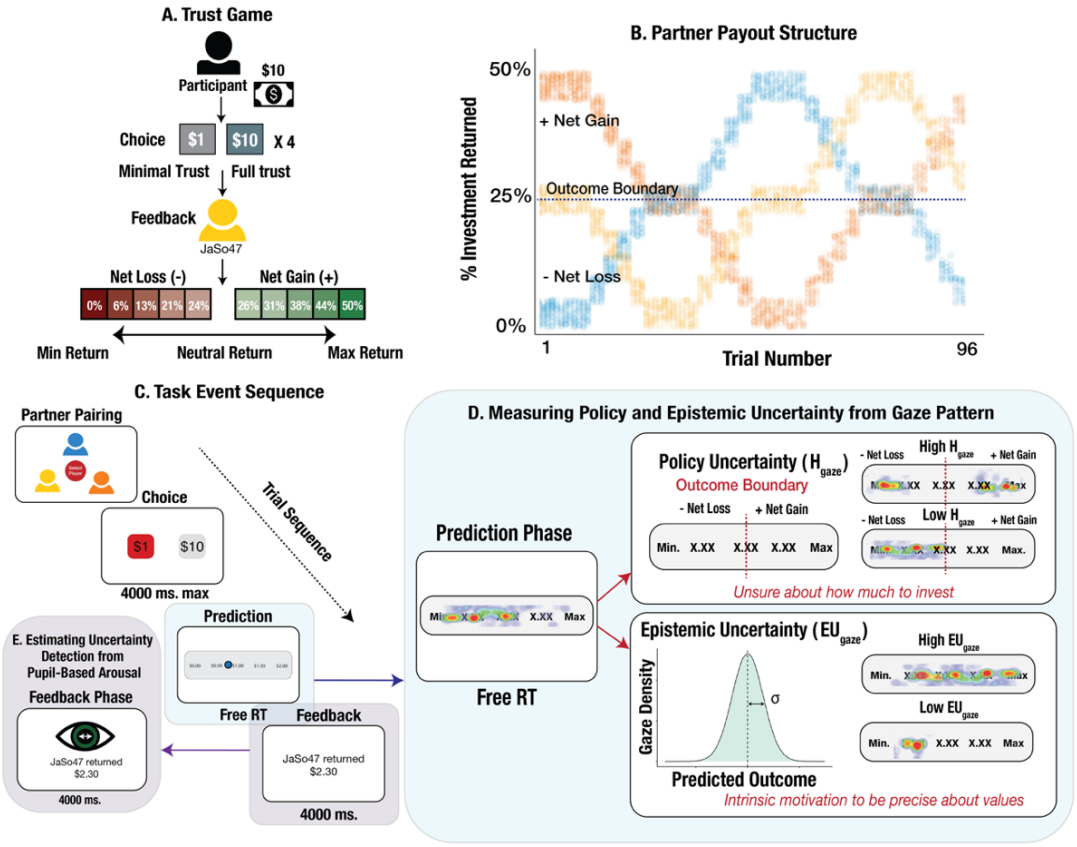

Figure 1. Experimental design and eye-tracking method to empirically estimate uncertainty. A. *Trust game. At the start of each trial, participants were paired with one of three presumed online partners, and could invest $1 or $10. The invested money is then quadrupled in value, and the partner receives the quadrupled sum. Partners then decide to return anywhere from 0-50% of the investment such that participants can lose all of the initial investment (0% return), double their investment (50% return), or receive any outcome in between.* ***B.*** *Partner payout structure. Social partners gradually reversed their payouts, requiring participants to continually adjust their choice policy. The dotted black line denotes the outcome boundary determining the optimal policy to maximize returns: participants should invest maximally ($10) when partners return more than 25%, and minimally ($1) otherwise to avoid a monetary loss.* ***C.*** *Task event sequence. Trials commenced with a partner pairing phase in which the computer selected a partner for the current round (see Methods). Participants were then given up to 4 seconds to indicate their investment and then made a prediction about how much money they believed their partner would return, before observing trial outcomes.* ***D.*** *Measuring policy and epistemic uncertainty from gaze patterns. During the prediction phase, participants were instructed to align their eye gaze (signaled to them with a blue dot) to the anticipated trial outcome. The gaze pattern over values was used to construct estimates of policy and epistemic uncertainty. Policy uncertainty was assessed as the extent to which gaze patterns spanned both sides of the boundary determining the optimal policy, quantified by entropy (H_{gaze}, see Methods). Epistemic uncertainty was quantified by the variance in gaze patterns irrespective of the outcome boundary.* ***E.*** *Estimating uncertainty detection from pupil-based arousal. During the feedback phase, arousal was estimated from the % change in pupil diameter (PD) from baseline.*

Results

Gaze patterns reliably index distinct sources of uncertainty. Participants (N = 94) completed 96 trials of the Trust Game with three partners (Fig. 1, A to B). Unbeknownst to participants, these partners were preprogrammed, slowly drifting in their reward rate over the course of the task, thereby requiring participants to continually adjust their choice policy to optimize rewards, the amount of money a partner reciprocated back to the participant (Fig. 1B; see Methods). To obtain trial-level estimates of uncertainty, we asked participants to predict their partner's behavior (amount of money reciprocated) using a response bar which displayed all possible monetary returns (Fig. 1D). A blue dot on the screen corresponded to the participant's gaze, allowing participants to lock in their predictions of how much money their partners would return by moving the blue dot with their eyes to the predicted monetary outcome. This enabled us to use gaze patterns to evaluate participants' trial-by-trial expectations, and their experienced uncertainty about anticipated outcomes (Fig 1D)—which is thought to govern the rate of learning. We can further leverage these gaze patterns to obtain precise and highly granular estimates of both policy and epistemic uncertainty.

To estimate policy uncertainty, we borrowed insights from prior computational models that adjust learning as a function of policy uncertainty, quantified by entropy (*H),* over choice probabilities (Franklin & Frank, 2015) which reliably captures human choice data in the current task (Lamba et al., 2020; see below). We derived an analogous measure of policy uncertainty based on gaze patterns, quantified by computing the entropy of the proportion of gazes on either side of the outcome boundary (H_{gaze}). The midpoint—which we refer to as the *outcome boundary*—is not explicitly marked but acts as a psychological boundary indexing whether participants expect to earn or lose money on the current trial, thus determining whether they should invest or not. An increase in gaze fixations on both sides of the boundary indicates greater uncertainty about the optimal choice policy (Fig. 1D) and should thus increase learning rates. However, even when one might be relatively certain about what they should do in the task (e.g., invest maximally or minimally), they may still experience residual uncertainty about the specific outcomes on a given trial (i.e., *exactly* how much their partner will return), motivating the pursuit of epistemic knowledge. Epistemic uncertainty about how much money would be returned was quantified as the standard deviation in gaze patterns over the range of outcomes (EU_{gaze}), which captures the precision of one's predictions.

Using our gaze-derived uncertainty measures, we examined whether knowledge about the optimal choice policy (i.e., invest minimally or maximally with the current partner) captures the expression of distinct sources of uncertainty in the task. H_{gaze} was significantly greater on trials with sub-optimal investments (i.e., choices that were inconsistent with the optimal choice policy) compared to optimal investments (t = -6.77, p < .001). In contrast, epistemic uncertainty, EU_{gaze}, was greater on trials in which participants selected the optimal response, suggesting that participants instead expressed uncertainty about exact monetary outcomes once they knew the optimal choice policy (t = 10.26, p < .001). Although expressed policy and epistemic uncertainty were correlated (t = 18.37, p < .001; Fig. 2A), we also observed that policy versus epistemic can trade off with each other, suggesting these are also dissociable uncertainty signals (see Methods and Supplement for details about our eye-tracking procedure and methodological validation).

People dynamically reorient their attention towards policy and epistemic uncertainty signals. We next tested whether the physiological expression of policy and epistemic uncertainty depends on task demands, such that participants dynamically trade off reducing policy and epistemic uncertainty when learning about others. We separated trials into two different periods, depending on which type of uncertainty should be more salient at a particular moment. *Adjust Policy* periods occur when the amount of money returned by the partner has just crossed the outcome boundary. On these trials, one's prior choice policy no longer maximizes their earnings, and thus the policy needs to be revised, which naturally increases policy uncertainty (H_{gaze}). In contrast, *Exploit Policy* periods comprise trials where we expect learning to have stabilized (i.e., at the end of a window in which partners were consistently trustworthy or untrustworthy). In these time windows, participants have generally learned the optimal choice policy, and can therefore use this opportunity to resolve residual epistemic uncertainty about partners (EU_{gaze}). We observed just this: policy uncertainty was greater during the Adjust Policy periods, whereas epistemic uncertainty was greater during the Exploit Policy periods (uncertainty type × trial type interaction $t = 9.75$, $p < .001$; Fig. 2B), indicating that expressions of policy and epistemic uncertainty are not only dissociable, but they dynamically trade off as task demands change. To formally capture this trade-off, we quantified the relative difference between gaze-derived policy and epistemic uncertainty estimates on each trial ($\Delta\varepsilon_{gaze}$; Fig. 2C), yielding a signed variable that indicates whether policy or epistemic uncertainty dominates at that moment (+ $\Delta\varepsilon_{gaze:}$ H_{gaze} greater; - $\Delta\varepsilon_{gaze}$: EU_{gaze} greater). These findings indicate that people dynamically and spontaneously orient their attention towards distinct sources of uncertainty, allowing learners to both adjust their choice policy as partners change, and gather additional value-based information about others.

Pupil-based arousal reflects attentional switching between policy and epistemic uncertainty. If individuals flexibly switch between resolving policy and epistemic uncertainty, then this attentional reorientation should also be reflected in physiological correlates of arousal. To quantify trial-level estimates of physiological arousal, we measured the % change in pupil diameter (PD) from baseline at the time of feedback (Fig. 1E; see Methods). We then assessed whether arousal is predicted by H_{gaze} and EU_{gaze}, including both in the same model to compete for variance. Moreover, we tested whether these relationships dynamically change based on knowledge of the optimal choice policy (i.e., which source of uncertainty should be more salient at a given moment). When participants were unsure of the optimal choice policy, H_{gaze} influenced pupil-based arousal (Beta coefficients for H_{gaze} were significantly greater on trials with high vs. low policy uncertainty: $t = -4.84$, $p < .001$; Fig. 2D). Conversely, when participants had a reliable estimate of how much their partner was going to reciprocate (i.e., policy uncertainty was low), EU_{gaze} exerted a stronger influence on pupil-based arousal ($t = 5.27$, $p < .001$), and the effect of H_{gaze} was suppressed. These findings reveals that each uncertainty form is also reflected in the physiological arousal system, providing a biological basis for adaptive prioritization that influences learning.

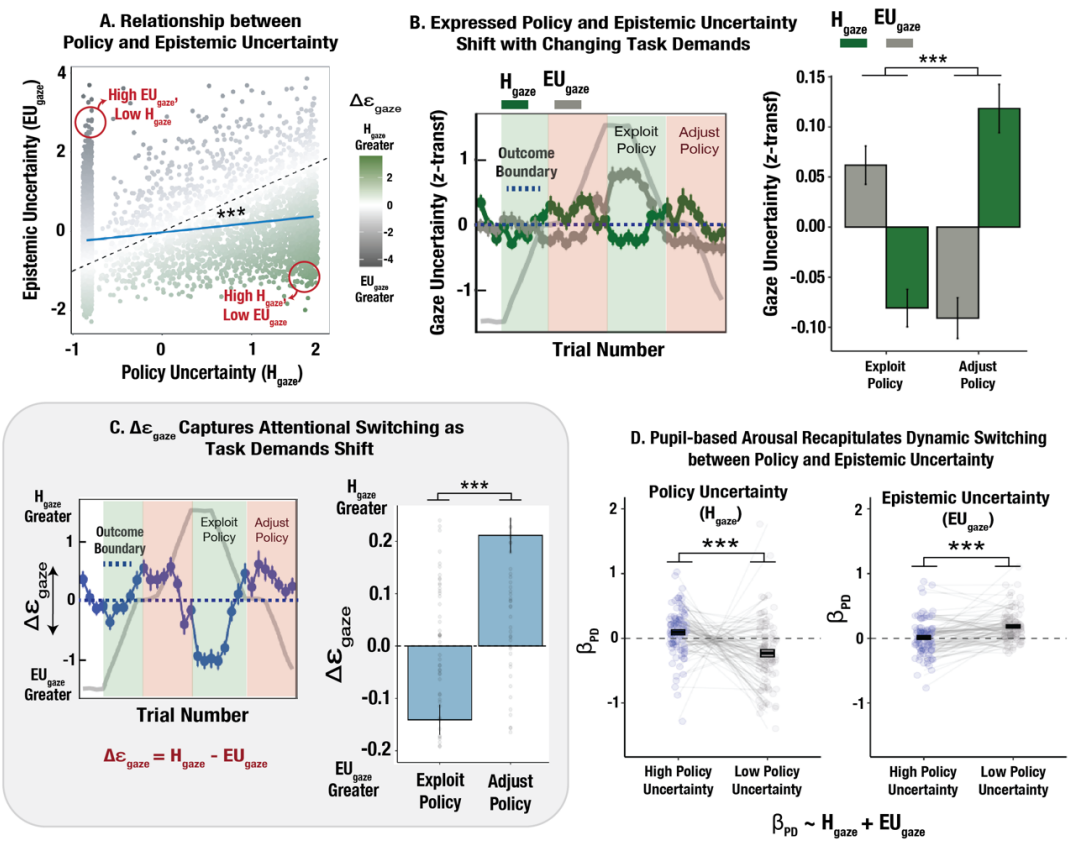

Figure 2. Expressions of uncertainty and pupil-based arousal dynamically adjust with changing task demands. ***A.*** *Relationship between gaze-derived policy and epistemic uncertainty measures.* H_{gaze} *and* EU_{gaze} *were positively correlated in the task, however, some trials were also characterized by a distinct trade-off in which either* H_{gaze} *or* EU_{gaze} *dominated. Points, corresponding to individual, trial-level measurements of policy and epistemic uncertainty are shaded based on the relative difference between policy and epistemic uncertainty,* $\Delta\varepsilon_{gaze}$. ***B.*** *Expressed policy and epistemic uncertainty shift with changing task demands. Left panel shows mean estimates of policy and epistemic uncertainty dynamically oscillate depending on whether prior choice policies could be exploited or needed to be adjusted. Results for one example partner type are shown. Right panel shows mean estimates of each type of uncertainty aggregated across all partner types.* ***C.*** $\Delta\varepsilon_{gaze}$ *captures attentional switching as task demands shift. The difference between* H_{gaze} *and* EU_{gaze}*, as a signed variable,* $\Delta\varepsilon_{gaze}$*, captures the relative magnitude of each uncertainty signal as partners change (*$t = 11.65$, $p < .001$*).* ***D.*** *Pupil-based arousal recapitulates dynamic switching between policy and epistemic uncertainty. Arousal measured as change in pupil diameter (PD) captures switching pattern between policy and epistemic uncertainty. When participants were unsure about their choice policy, PD was predicted by* H_{gaze} *and not by* EU_{gaze}*. Conversely, when participants were confident about their current choice policy, PD was no longer predicted by* H_{gaze} *and instead was predicted by* EU_{gaze}*, thus physiologically reflecting the dynamic switching between each form of uncertainty. Individual points correspond to participant beta coefficients from the regression model. Asterisks (*,**,***) denote* $p < .05$, $p < .01$, $p < .001$*, respectively. Errors bars indicate the standard error of the mean.*

Anxiety impacts ability to swiftly resolve policy uncertainty. Individual variability in tolerance of uncertainty is likely to impact how humans attend to and expediently resolve uncertainty signals. We used recommended clinical significance cut-offs on two trait anxiety scales (see Methods), yielding approximately evenly sized high and low anxiety groups ($N_{low\ anxiety}$=45, $N_{high\ anxiety}$=49). Replicating our prior results (Lamba et al., 2020), we observed that highly anxious participants invested significantly more money on loss blocks (i.e., when partners were untrustworthy) compared to the low anxiety group (untrustworthy-start partner: valence × group interaction, t = -2.53, p = 0.011; trustworthy-start partner: valence × group interaction, t = -2.74, p = .0062; Fig. 3A).

We next evaluated whether anxiety impacts how effectively individuals resolve policy and epistemic uncertainty when learning about others. Comparing $\Delta\varepsilon_{gaze}$ (i.e., the relative weighting between policy and epistemic uncertainty) across all trials, high anxiety participants generally expressed greater policy uncertainty relative to epistemic uncertainty, whereas the low anxiety group demonstrated the opposite pattern, instead expressing more epistemic uncertainty (t = 2.89, p = .0038; Fig. 3B). This pattern suggests that the high anxious group experienced greater difficulty identifying the optimal choice policy in the task, whereas the low anxiety group was able to swiftly resolve policy uncertainty but remained more unsure about exact monetary outcomes from trial to trial. Moreover, although both groups expressed greater policy uncertainty when engaging with untrustworthy compared to trustworthy partners (t = -5.76, p < .001; Fig. 3C) which suggests it is was more difficult to learn the optimal policy in the loss domain, this effect was exacerbated in the high anxiety group (t = 2.69, p = .0073). Thus, comparing patterns of policy and epistemic uncertainty in the task, we find that the anxious group was more unsure of the optimal choice policy whereas the low anxiety group was more unsure about epistemic knowledge, indicating that these groups differentially prioritize which type of uncertainty signal to resolve.

Anxious individuals show intact physiological arousal to epistemic uncertainty and blunted detection of policy uncertainty. Two common threads emerge across our behavioral and gaze-based analyses. First, we find that highly anxious participants are slower to behaviorally adapt to increasingly untrustworthy partners. Second, we find that the relative expression of policy and epistemic uncertainty is altered in anxious individuals, particularly in the loss domain. It remains unclear, however, whether slower adaptation to untrustworthy people occurs because anxious participants fail to detect policy uncertainty writ large or because they maladaptively respond to policy uncertainty. With the latter, maladaptive responding could be a function of persistently enhanced physiological arousal, or, enhanced prioritization of epistemic knowledge. To test these competing hypotheses, we correlated our gaze-based measures of policy and epistemic uncertainty with pupil-based arousal during the feedback phase. As demonstrated in prior work, increased pupil-based arousal during feedback indexes the magnitude of surprise elicited from outcomes and the rate of learning adjustment (Nassar et al., 2012). By linking policy and epistemic uncertainty with pupil-based arousal, we can identify the extent to which each source of uncertainty serves as a distinct physiological update signal in high and low anxiety groups.

Across both groups, greater epistemic uncertainty (EU_{gaze}) was positively correlated with pupil-based arousal (t = 3.88, p < .001; Fig. 3D), indicating that both groups exhibited increased physiological arousal to outcomes when they were unsure of *exactly* how much partners would return. In contrast, we observed a significant interaction between policy uncertainty and anxiety level on pupil-based arousal, such that the effect of policy uncertainty (H_{gaze}) on pupil dilation was selectively suppressed in the high anxiety group (H_{gaze} × group interaction: t = -2.13, p = .0336; Fig. 3D). That is, in addition to experiencing greater difficulty resolving policy uncertainty, anxious individuals also showed reduced physiological arousal when their policy uncertainty increased, the opposite effect to what was observed in the low anxiety group. Moreover, whereas low anxiety participants demonstrated the predicted pattern of increased arousal after partners' behaviors crossed the outcome boundary, indicating that the choice policy should be updated, highly anxious participants demonstrated reduced arousal during this same time period (policy period × group interaction: t = -3.12, p = .0012; Fig. 3E). These effects were further modulated by valence, such that the low anxiety group exhibited increased arousal when engaging with increasingly untrustworthy partners (policy period × valence interaction: t = -2.39, p = .0169; Fig. 3F), whereas the high anxiety group generally reduced arousal when partners were untrustworthy (main effect of valence: t = 2.79, p = .0053). Thus, the arousal pattern from our pupillometry measures suggests that reduced learning from losses in the anxiety group arises, in part, from a failure to promptly detect and respond to changes in policy uncertainty, while physiological detection of epistemic uncertainty remains unaltered.

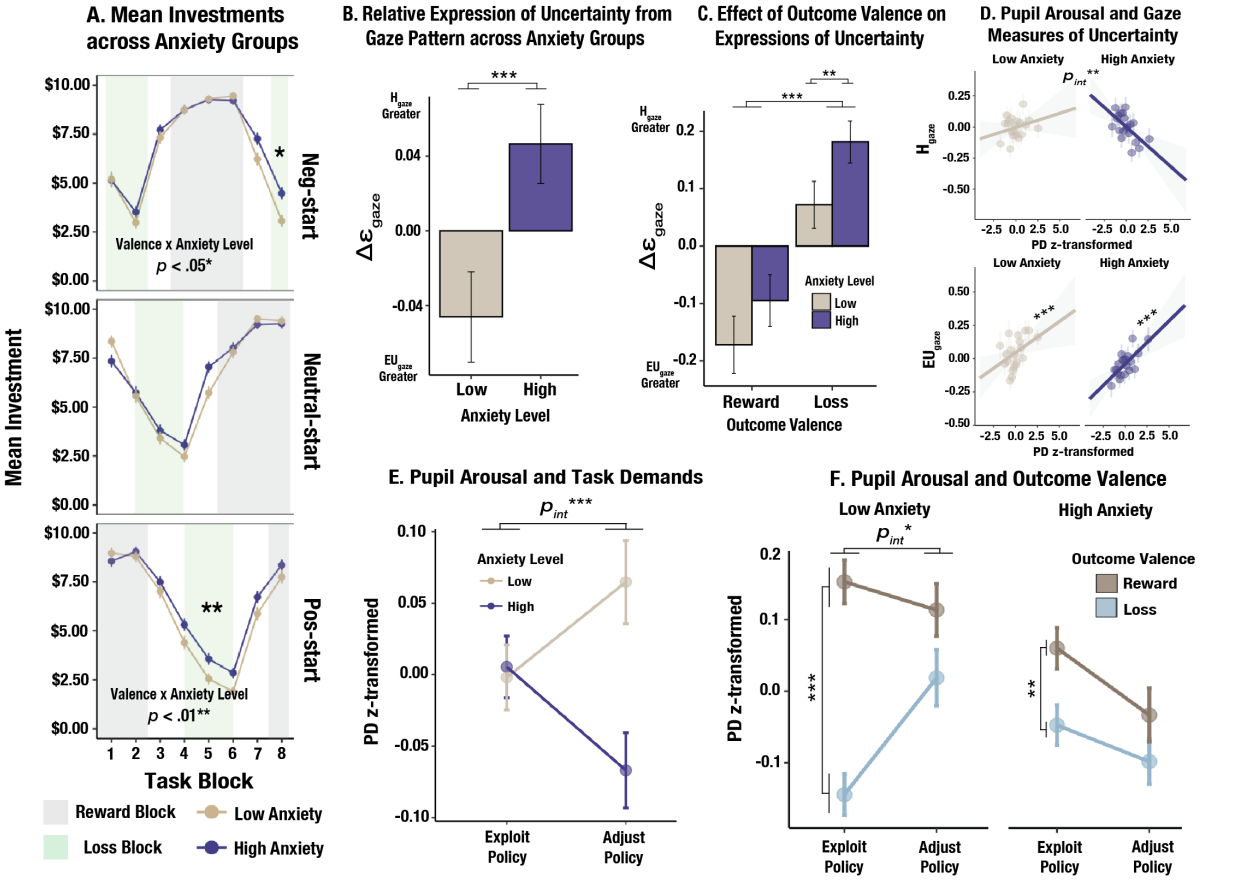

Figure 3. Impact of anxiety levels on expressions of uncertainty and pupil-based arousal. A. *Mean investments across anxiety groups. The high anxiety group invested significantly more money with partners that were untrustworthy leading to greater monetary losses compared to the low anxiety group. Asterisks correspond to valence × group interaction effect for each partner type.* ***B.*** *Relative expression of uncertainty from gaze pattern across anxiety groups. Across all trials, the high anxiety group expressed more policy uncertainty compared to the low anxiety group, suggesting that they spent more time being unsure of the optimal choice policy in the task.* ***C.*** *Effect of outcome valence on expressions of uncertainty. Both groups experienced more policy uncertainty on loss trials, however, this effect was greater in the high anxiety group.* ***D.*** *Pupil-based arousal and gaze measures of uncertainty. H_{gaze} was associated with increased physiological arousal in the low anxiety group but suppressed arousal in the high anxiety group. *** Denotes the anxiety group × trial type interaction effect. In contrast, EU_{gaze} predicted increased arousal in both groups. For visualization in both correlation plots, data from each trial was binned into z-transformed pupil diameter (PD) intervals along the x-axis, for each 5fth percentile PD increment. Statistics were conducted using the raw, un-binned PD measures.* ***E.*** *Pupil arousal and task demands. The low anxiety group showed increased arousal during the Adjust Policy Period after partners changed, whereas the high anxiety group showed suppressed arousal when choice policies needed to be adjusted.* ***F.*** *Pupil arousal and outcome valence. The low anxiety group showed increased arousal when partners suddenly became untrustworthy. * Denotes the outcome valence × trial type interaction effect on pupil arousal in the low anxiety group, *** Denotes the main effect of valence. In contrast, the high anxious group showed reduced arousal when partners were suddenly untrustworthy. Asterisks (*,**,***) denote $p < .05$, $p < .01$, $p < .001$, respectively. Errors bars indicate the standard error of the mean.*

Computational modeling reveals asymmetric reductions in learning from social losses vs. rewards in the anxious group. Flexibly resolving policy and epistemic uncertainty guides successful learning in a dynamic environment—a process that is disrupted by anxiety. To examine the mechanistic link between these uncertainty signals and the rate of learning adjustment we used a computational modeling approach. We tested and compared three Bayesian Reinforcement Learning models (BRL; see Methods). Our core model, Dynamic-BRL (DBRL), was developed in our prior work (Lamba et al., 2020) in which trial-level beliefs are adjusted through outcome history. As a Bayesian learner accumulates evidence that a partner is (un)trustworthy, it becomes more confident in that belief. Thus, when a partner changes their behavior, such a model will overly rely on the history of prior outcomes (Daw et al., 2005; Doll et al., 2009). To capture how the effect of prior outcomes on posterior beliefs should be adjusted in a nonstationary environment, our dynamic Bayesian model leverages changes in policy uncertainty to modulate decay (i.e., forgetting). By dynamically decaying prior beliefs as policy uncertainty increases, one can prioritize learning from more recent outcomes and quickly accumulate evidence, allowing new choice policies to form. Thus, rather than assuming a constant probability of change at a fixed rate, decay increases when the agent becomes more uncertain about what to do, thereby balancing the tradeoff between stability and flexibility (Franklin & Frank, 2015). Here, policy uncertainty is calculated as the entropy, H, over the agent's choice probabilities, where p_1 and p_2 refer to the agents probability of investing maximally ($10) or minimally ($1), respectively. Notably the analogous formulation of H was used to calculate our gaze-derived estimate of policy uncertainty, H_{gaze} (see Methods).

$$H_t = -[p_1 \times log_2(p_1) - p_2 \times log_2(p_2)]$$

Consistent with our previous model for this task, decay was modeled separately for gains and losses (γ_{pos} and γ_{neg} respectively). We further deconstructed γ into a constant γ_0 term (baseline beliefs about changeability) and a separate γ_1 term to allow decay to further increase or decrease as a function of the learner's change in policy uncertainty from trial to trial, quantified by *ΔH*. Note that in our prior work, we constrained γ_1 to negative values, reflecting the assumption that as policy uncertainty increases, prior values are decayed. In our current model, DBRL-2, we relaxed this assumption and allowed changes in policy uncertainty to either decay prior reward history *or* exert the opposite effect of preserving prior knowledge (see Methods), allowing us to better capture the behavioral profile of anxious participants who show reduced learning when policy uncertainty increases.

$$\gamma_{pos} = \gamma_{0_{pos}} + \gamma_{1_{pos}} \cdot \Delta H$$
$$\gamma_{neg} = \gamma_{0_{neg}} + \gamma_{1_{neg}} \cdot \Delta H$$

Across both high and low anxiety groups, the DBRL-2 model best captures behavior, outperforming our prior model (pxp > .99; see Methods and Supplement for model comparison details), and could reliably reproduce participant choices (see MLE model simulation, Fig 4A). To validate that policy uncertainty estimates from the model (*H*) were generally consistent with our gaze-based policy uncertainty measures (H_{gaze}) we examined the overall profile of trial-level *H* patterns from the model. Mirroring the physiological gaze-based analyses (Fig. 2C), model-estimated *H* was greater during the adjust versus exploit policy period when choice policies need to be revised (t = 5.02, p < .001; Fig. 4B). Further, model-estimated H also recovered valence-dependent policy uncertainty differences across high and low anxiety groups (valence × anxiety group interaction*:* t = 6.31, p < .001; Fig. 4C). Specifically, model-estimated policy uncertainty was lower for losses in the high anxiety group, indicating less behavioral variability (i.e., perseveration) when partners are untrustworthy. Thus, entropy estimates derived from both our computational model and from our eye-gaze measures provide a converging picture of increased policy uncertainty when the environment changes (i.e., when partners cross the outcome boundary), and disrupted resolution of policy uncertainty for those with increased anxiety.

Comparing decay parameters from the winning DBRL-2 model, we observed a significant difference in baseline decay, γ_0, across groups in the loss domain (valence × anxiety group interaction: t = -2.33, p = .0219; Fig. 4D), revealing a learning asymmetry in the anxious group for gains vs. losses. To further probe how a learning asymmetry maladaptively biases behavior in the task, we next asked whether anxious participants might employ a consistent policy (i.e., maintain trust) to simply learn more about their partners. That is, when partners are trustworthy and one's choice policy can be safely exploited, anxious individuals might prioritize gathering epistemic information by learning *exactly* how trustworthy their partner is at the expense of adjusting their choice policy, even as policy uncertainty increases (i.e., a partner crosses the outcome boundary). Such a finding would accord with our pupil results suggesting that intact arousal gates the detection of environmental changes by signaling the need to adjust one's policy—a process that is perturbed in the high anxiety group while physiological responsivity to epistemic uncertainty remains intact.

Anxious individuals prioritize epistemic knowledge over optimizing their choice policy. To test the explicit prioritization of epistemic knowledge over policy optimization in the high anxiety group, we evaluated whether the degree of epistemic uncertainty (EU_{gaze}) during the Exploit Policy period (i.e., periods in which participants could focus on gathering value-based information about trustworthy partners) predicted task performance after partners crossed the outcome boundary and became untrustworthy. To obtain estimates of trial-to-trial updating using the DBRL-2 model, we calculated the Kullback Leibler Divergence (KLD) as an index of distance between the choice policy of a perfectly optimal learner—a Bayesian agent that efficiently maximizes monetary outcomes—and participant estimates of the optimal choice policy, taking one's prior outcome history into account. We observed a significant group × EU_{gaze} interaction (t = -2.56; p = .0123; Fig. 4E), such that in the high anxiety group, an increased focus on gathering epistemic knowledge during the exploit policy period predicted slower behavioral adjustment after partners crossed the outcome boundary. These findings suggest that people with increased anxiety show a bias towards figuring out *exactly* how trustworthy partners are rather than optimizing their choice policy, thus resulting in maladaptive behavior.

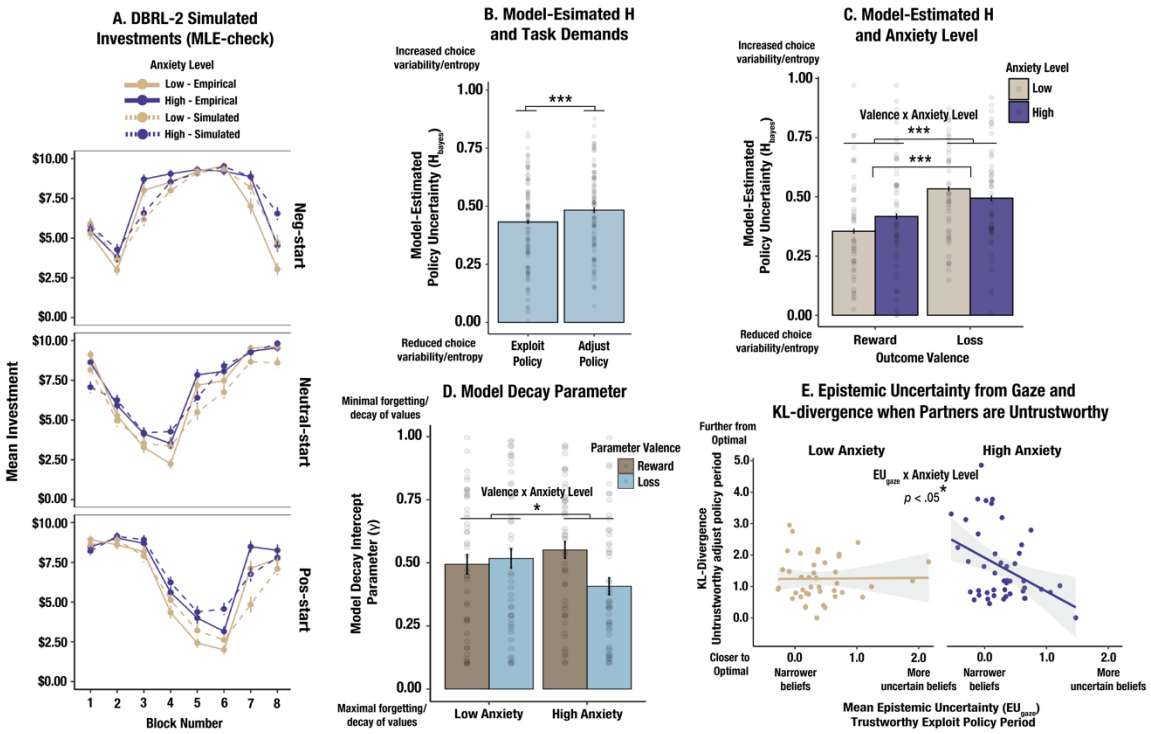

Figure 4. Dynamic Bayesian-RL model shows that anxious individuals are slower to adapt to untrustworthy partners. ***A.*** *DBRL-2 simulated investments from MLE-check. Data was simulated using each participant's MLE-optimized (i.e., best-fitting) parameters. Model-simulated data recapitulates learning differences between groups.* ***B.*** *Model-estimated H and task demands. Model estimates of policy uncertainty (H) increase when choice policies need to be adjusted consistent with the pattern observed from our gaze-derived policy uncertainty estimates.* ***C.*** *Model-estimated H and anxiety levels. High anxiety participants show reduced, rather than increased policy uncertainty (H) on loss trials, the opposite pattern from what we observed empirically (Fig. 2C), indicating that as highly anxious participants physiologically express more policy uncertainty (H_{gaze}) their choice variability decreases as assessed by model-estimated H.* ***D.*** *Model decay parameter. The gamma intercept (γ_0) captures baseline beliefs about changeability. Highly anxious individual exhibit a valence-specific learning asymmetry towards preserving previously learned rewarding values and having more uncertain beliefs (i.e., priors) when partners are untrustworthy, an asymmetry that produces a tendency to overinvest with untrustworthy partners. * Denotes the valence x anxiety group interaction.* ***E.*** *Epistemic uncertainty from gaze and KL-divergence when partners are untrustworthy. KL-divergence indexes optimal updating while taking one's prior observed outcome history into account. In the high anxiety group, participants with more confident beliefs about trustworthy partners (i.e., reduced epistemic uncertainty) exhibit worse performance (i.e., less optimal updating) after partners changed course and became untrustworthy. Asterisks (*,**,***) denote $p < .05$, $p < .01$, $p < .001$, respectively. Errors bars indicate the standard error of the mean.*

Discussion

Adaptively functioning in our social world requires integrating across multiple sources of uncertainty so that we can expediently refine our beliefs and behaviors. Prior work investigating the influence of uncertainty on learning typically examines uncertainty along a single dimension (Mathys et al., 2014; Nassar et al., 2010; Siegel et al., 2018), limiting our knowledge of how different types of uncertainty either independently or jointly inform learning. We developed a novel eye-tracking procedure premised on information sampling theories that granularly teases out each source of uncertainty in real time. Our study reveals two key findings: People dynamically reorient their attention towards each source of uncertainty as social interactions unfold, and this attentional flexibility is critical for adaptive learning. In contrast, people with high anxiety show inflexible attentional switching. This inflexibility is characterized by reduced attention to policy uncertainty, but intact responsiveness to epistemic uncertainty. Although policy optimization is necessary to improve task performance, those with anxiety choose to gather information about other people, rather than take action. These findings advance our knowledge from prior work which has historically only considered the effect of a single source of uncertainty on learning and has typically only examined learning in nonsocial contexts. Further, while our findings dovetail with prior work showing that highly anxious people learn less from uncertain outcomes (Aylward et al., 2019; Browning et al., 2015; Gagne et al., 2020; Lamba et al., 2020), we show that anxiety is not associated with a blanket uncertainty insensitivity. Rather, anxiety is characterized by a biased uncertainty filter.

Our work also sheds new light on the fundamental limitations of exclusively relying on policy or valued-based accounts when evaluating learning and decision-making processes in complex, naturalistic environments. While prior neural evidence suggests that striatal dopamine contributions to learning are policy-based (Coddington et al., 2023; Jaskir & Frank, 2023; Li et al., 2011; Li & Daw, 2011), and prefrontal contributions are value-based (Boorman et al., 2013; Frank & Claus, 2006; Hare et al., 2008; Rushworth & Behrens, 2008) , little work to date has extensively considered interactions between these systems. Here we show that the value of a particular uncertainty signal for learning must be dynamically contextualized within the demands of the task and the learning goals of the agent. Specifically, in our task we focused on one particular mechanism by which policy and epistemic signals interact, namely by dynamically switching attendance to each uncertainty source as new learning demands arise. Future work should consider how the functional utility of adjusting one's attention towards epistemic knowledge or adjusting one's policy might be governed by prefrontal systems (i.e., a hypothetical meta-critic; Jaskir & Frank, 2023) conveying the prioritization of uncertainty signals to solve a particular problem, and how biases in this system might alter learning.

Previous work has also linked unexpected events to increased norepinephrine release in the locus coeruleus and phasic changes in pupil dilation (Aston-Jones & Cohen, 2005; Rajkowski, 1993; Yu & Dayan, 2005). As uncertainty in the environment increases, increased pupil-based arousal governs the rate of learning adjustment, allowing learners to quickly adapt (Nassar et al., 2012, 2019). In the current work, we provide novel evidence that multiple uncertainty signals influence pupil-based arousal, and this relative influence dynamically adjusts with changing learning demands. Future work should explore how norepinephrine release impacts policy selection in the basal ganglia and value-based signals in the prefrontal cortex, perhaps by biasing the prioritization

and salience of policy optimization and epistemic-oriented motivations. While prior work has demonstrated that the coupling between pupil-based arousal and uncertainty detection is disrupted with increased anxiety (Browning et al., 2015), we provide new evidence that this relationship is dependent on the *source* of uncertainty. While anxious individuals show reduced physiological sensitivity to policy-based uncertainty signals, responsivity to epistemic uncertainty remains unaltered.

Last, our eye-tracking procedure, which dissociates between different forms of uncertainty in real-time, allows us to evaluate whether altered learning might arise from individual variability in attending to distinct sources of uncertainty. While prior work speculates that reduced learning from losses in people with anxiety might arise from disrupted learning under uncertainty (Aylward et al., 2019; Browning et al., 2015; Gagne et al., 2020), here we offer a different explanation—one in which the balance in learning from a specific type of uncertainty is reconfigured such that one source of uncertainty can be overly prioritized in the system (i.e., epistemic knowledge), leaving other forms of uncertainty that are critical for task performance unresolved (i.e., policy uncertainty). This account leaves open a new perspective in computational psychiatry approaches towards understanding anxiety-based disorders—one in which disrupted learning and decision-making might reveal a divergent and heterogenous set of goals and motivations of the learner.

Methods

Participants. The study protocol was approved by Brown University's Institutional Review Board (Protocol #1607001555). All participants indicated informed consent prior to behavioral and eye-tracking data collection. Participants (N = 100, N_{female} = 47, N_{male} = 53, mean age = 20.41) were recruited from the subject research pool (SONA) managed by the Cognitive and Psychological Sciences Department at Brown University in Providence, Rhode Island. All participants received either monetary compensation ($15/hour) or course credit, including additional performance-based bonus payment of up to $20. After data collection, 6 participants were excluded from final analyses because they did not adequately perform the task (i.e., no behavioral variability in the choice data), or due to poor gaze and pupil readout from the eye-tracker in which more than 50% of trials contained signal dropout. One participant stopped the experiment halfway through the session due to illness. Our final sample consisted of 94 participants from which we obtained behavioral, physiological, and clinical data. All participants indicated normal or corrected vision and no prior history of neurological injury that would impact gaze range.

Evaluating Anxiety. Participants were grouped as a function of low and high anxiety levels based on their responses from the 7-item Generalized Anxiety Disorder Scale (GAD-7) and the State-Trait Anxiety Inventory (STAI). Our low and high anxiety groups are based on established clinical guidelines, in which a score of 10+ on the GAD-7 scale (Löwe et al., 2008; Spitzer et al., 2006) and a score of 40+ on the trait component of the STAI scale (Spielberger, 1983) are considered reliable predictors of pathological anxiety (i.e., anxiety that is disruptive to one's daily functioning and/or well-being). For our statistical analyses of group differences, participants were placed into the high anxiety group if they were above the significance cutoff on one or both anxiety inventories, and into the low anxiety group if they were below the cutoff on both the GAD-7 and STAI scale. Based on these criteria, our sample was split into roughly evenly sized high and low anxiety groups ($N_{low\ anxiety}$ = 45, $N_{high\ anxiety}$ = 49). Note, assessed anxiety levels in our study does not evaluate whether participants meet the criteria for a DSM-5 generalized anxiety disorder.

Task stimuli. The task was presented using Psychtoolbox-3 for MATLAB. Prior to data collection, participants were instructed that they would be paired with three different online partners to play a game with, in real time. In actuality, partners were programmed agents set to return predetermined reward rates (see below). Participants were not given any prior knowledge about their partners' identity, such as gender, age, or geographical location. Each participant was assigned a username to represent their identity, which consisted to the first two letters of their first name, the first two letters of their last name, and two numbers of their choosing (e.g., OrFe95). Partner identifies were reciprocally displayed to participants as usernames, with the same three partner identities (AmLa55, KeJo93, JaSo47) assigned to each partner across experimental sessions. Each partner was represented as a distinctly colored avatar (blue, yellow or orange).

Task reward structure. Each partner was randomly assigned to a follow a pre-programmed and distinct outcome trajectory, starting out initially trustworthy, untrustworthy, or neutral and then gradually reversing over the course of the task (Fig. 1B). On each trial, partners were set up to return a fixed proportion of the invested money between 0-50% (e.g., 25%), with a uniform 5% noise interval around this return rate. For example, if the agent was set to return 25% of the initial investment, the computer randomly selected a value between 22.50-27.50%, which determined the

actual amount on that trial. Trials with each partner type elapsed over alternating stable and drifting blocks, with each block consisting of 4 trials per partner type. During stable blocks, the mean return rate stayed fixed for the duration of the block (with some noise around the actual returns). In contrast, partners increased or decreased their mean return rate by 4% on each trial during drifting blocks, requiring participants to keep close track of their returns. On a subset of these drifting blocks, the partner's return rate crossed the 25% outcome boundary, such that they were now returning less than 25% or more than 25%. This change was thus consequential for participants because it would have required an adjustment in one's choice policy (i.e., strategically invest $1 or $10 with this partner) in order to maximize payoffs. Thus, we refer to these blocks as *Adjust Policy Periods.* The experiment also consisted of trial blocks which we refer to as *Exploit Policy Periods,* in which participants could continue using their current investment strategy with no consequence to their current payoffs (assuming they figured out the optimal choice), even if partners were drifting. This design therefore allowed us to fully cross partner outcome valence (i.e., whether trials resulted in net gains or losses) with partner stability so we could systematically examine their distinct effects on learning.

Task sequence. Participants completed 32 rounds of the Trust Game with each partner in rotating trial order (96 trials total), such that they interacted with each partner once every three trials (example trial ordering: 1,2,3,2,3,1,1,3,2,3,1,2). Pseudo-random trial ordering was chosen to reduce the temporal distance between exposures to each stimulus. A unique trial ordering was generated for each participant within the task program. Each trial consisted of four distinct phases: partner pairing, choice, prediction, and feedback. Behavioral data was collected during the choice phase, and physiological measurements were collected during prediction and feedback (see eye-tracking section below).

Partner pairing. At the onset of the partner pairing phase, participants were shown the identities of the three partners in a triangular configuration. To avoid task and vision fatigue, participants were given a "select partner" button placed in the center of the screen which initiated the trial sequence whenever participants were ready to begin. Note, participants were not given the option of selecting their partner (they were paired with a partner as described above). The purpose of the select partner button was to indicate when participants were ready to begin the trial, thus allowing for short rest periods between trials as needed. After the spacebar was pressed, there was a brief 2-4 sec. jittered delay while the computer "paired" participants with a partner.

Choice. During the choice phase, participants were shown two choice options, $1 and $10, presented in white boxes on the left and right side of the screen, respectively. Responses were selected using the "f" and "j" keys, with a decision deadline of 4 secs. If a response was not made within the 4 sec. time window, a "MISSED TRIAL" prompt appeared on the screen and participants were immediately taken to the feedback screen which indicated a $0 outcome.

Prediction. After the choice phase, participants indicated their beliefs about the current trial outcomes using a horizontal bar which filled the width of the screen (Fig. 1D). The bar served as a guide for indicating one's predictions and was marked with 5 equidistantly spaced monetary values. The minimum value on the prediction bar (furthest left) was always $0, as this was the lowest amount that could be returned to the participant, and the maximum value (furthest right) was either $2 or $20 depending on whether the participant invested $1 or $10, respectively. The midpoint on the bar, which we refer to as the *outcome boundary*, corresponded to exactly what the participant invested (i.e., $1 or $10), and thus represented a $0 net gain or loss. This partitioned the bar into two sections—the left side of the outcome boundary which displayed predicted

monetary losses, and the right side which displayed predicted earnings. The intermediate monetary values on the response bar were evenly spaced intervals between the minimum and maximum values (e.g., $0, $0.50, $1.00, $1.50, $2.00).

Gaze-contingent display showed participants their gaze location in real time, which was indicated with a blue dot. Participants were instructed to align the blue dot to the point on the bar that was closest to the predicted trial outcome and were encouraged to also consider values in between the marked intervals. Once they were satisfied with the placement of the blue dot, they were instructed to hit the spacebar. Accuracy during the prediction phase was non-incentivized and there was no finite response deadline, allowing us to capture one's intrinsic motivation to precisely predict trial outcomes (i.e., reduce epistemic uncertainty).

Feedback. Following the prediction phase, participants were shown the outcome of the current trial. Before the actual outcome was displayed, the text displaying the numeric trial outcome was occluded (e.g., JaSo47 returned $XX.XX), for a 1 sec. duration, allowing us to measure pupil size at baseline before the trial outcome were presented. After the 1 sec. baseline calibration period, the filler text, $XX.XX, was replaced with the actual monetary outcome (e.g., JaSo47 returned $9.50), allowing us to control for luminance artifact in the pupil measurement when feedback was displayed. Pupil size was measured for a fixed 3 second period on each trial during which the trial outcome remained on the screen.

Eye-tracker and drift correction. Gaze location and pupil diameter were simultaneously measured using the Eyelink 1000 infrared camera (SR Research; Ottawa, Ontario) at a sampling frequency of 1000 Hz (1000 samples per second). Participants used a chin rest, which was placed approximately 80 cm away from the display screen (44 cm length × 37 cm width). Gaze location was measured and recorded from the left eye in pixel units. As previous methodological papers have noted (Cornelissen et al., 2002; Holmqvist et al., 2012), infrared eye-trackers are susceptible to drift shift in which measured gaze location will gradually deviate from actual gaze location over time. In line with manufacturer recommendations, all participants completed the standard Eyelink 9-point gaze calibration routine prior to data collection, ensuring that all recorded gaze samples were within 10 pixels of true fixation coordinates. However, because the nature of our task required very precise gaze measurements, particularly along the prediction bar, we implemented a custom drift correction procedure at the start of each trial to accommodate for additional drift over the course of the experiment.

Custom drift correction routine. To evaluate drift from trial to trial, participants were asked to directly fixate on a cross (+) displayed on the screen for a 2 sec. duration, without blinking if possible. Following fixation, drift correction was applied if the recorded gaze location deviated from the location of the fixation cross. Gaze recordings along x and y coordinates were adjusted based on the recorded deviation from fixation ($x_{corrected} = x + d_x$, $y_{corrected} = y = d_y$), where d_x and d_y are the computed distance between gaze measurements and fixation along x and y coordinates. Drift correction parameters were then tested during a 1.5 second test phase in which participants were instructed to continue to fixate on the cross while a gaze-contingent blue dot appeared on the screen. The blue dot aligns precisely with the fixation cross when drift shift is accurately computed. Drift correction was repeated if the computed drift was greater than 30 pixels away from the fixation cross in any direction after drift correction was applied. Gaze was recalibrated using the Eyelink 9-point routine if drift could not be corrected within 30 pixels of precision after two tests. This strict drift correction procedure ensured highly precise gaze recordings and allowed participants to reliably control the gaze-contingent blue dot with ocular movements.

Data preprocessing. Gaze and pupil data were preprocessing in MATLAB 2017a using custom scripts in the following steps: signal dropout identification, downsampling, linear interpolation. Preprocessing steps were completed separately for each phase in task. Trials with more than 50% signal dropout (i.e., more than 50% of returned eye-tracker samples were null) were omitted from further analysis. For ease of analysis, all remaining data was then downsampled from 1000 to 100 Hz. As an exception, data from the prediction phase was kept at a higher sampling frequency to ensure we had sufficient gaze samples to calculate entropy from saccades (see below) and was instead downsampled to 500 Hz. Downsampling was implemented by binning data to yield the desired number of samples per second and averaging the samples within each bin. Linear interpolation was then used to correct for blinks (Siegle et al., 2008) that occurred during the feedback phase and was only applied to pupil data. Based on prior findings that pupil diameter temporarily constricts and re-dilates before and after a blink, we expanded the interpolation window to 60ms prior and 150ms post blink, in line with recommendations (Siegle et al., 2008). We interpolated values within this time window using MATLAB's 1-D data interpolation function based on the samples before and after the interpolation period.

Evaluating arousal from pupil diameter during feedback. We used a baseline subtraction method to index arousal from pupil diameter during the feedback phase. Each feedback phase was trimmed into an event epoch including the 1 sec. baseline calibration period in which the trial outcome was occluded, followed by the feedback display period. To compute change in arousal from baseline, we indexed the first reliable pupil dilation estimate from the baseline calibration period in raw pupil area (pa) units. We then subtracted the baseline value from all subsequent raw pupil diameter measurements. To control for individual variability in average pupil size across participants, we converted raw pa to % change in pupil diameter from baseline using the equation below, where *i* indexes each eye-tracker sample post feedback onset. Pupil-based arousal as reported in our main text was simply the mean % change in pupil diameter from feedback onset to the end of the trial event epoch.

$$pa\ change_i = pa_i - baseline\ pa$$

$$\%\ pa\ change_i = \frac{pa\ change_i}{baseline\ pa} \times 100$$

Evaluating trial outcome predictions from gaze. We constructed trial-level estimates of one's outcome predictions and experienced uncertainty using the pattern of eye movements along the prediction bar. For each trial we created an event epoch for the duration of the prediction phase. Epochs were variable in duration as the prediction phase was self-paced. We next evaluated sampled prediction values along the bar, which could be identified from the pattern of fixations and saccades across the screen (see below). Fixations, broadly defined as stabilized locus of visual attention, vary in duration and frequency depending on a number of factors, such as the task (e.g., reading versus scene perception) and stimulus complexity (Carter & Luke, 2020). Generally, prior studies that have tested and analyzed several conventional fixation identification methods, such as dispersion and area-based algorithms, report that individual fixations are at least 100 milliseconds in duration (Salvucci & Goldberg, 2000). Saccades, the ballistic movements between fixation points (Carter & Luke, 2020), also vary in terms of duration and velocity depending on the nature

of the task, however, are widely reported to last approximately 30 milliseconds during reading and 40-50 milliseconds during scene perception (Carter & Luke, 2020). Our task required participants to use ocular movements to indicate anticipated outcomes along a bar, thus involving both lateralized and dispersed eye movements analogous to both reading and scene perception, suggesting that fixations and saccades in our task should be in a similar temporal range. To derive our prediction and uncertainty estimates we analyzed variation in gaze locations along the x-axis of the screen. Gaze coordinates were recorded in pixel units and were then mapped onto prediction values on a 925 x 231pixel prediction bar. Fixations which fell more than 30 pixels away from the edge of the bar were omitted from analyzes. Gaze coordinates, down-sampled to 500Hz, were then placed into 40 millisecond temporally contiguous bins and averaged together so that each gaze sample was no greater in length than a saccade.

Gazes were then range normalized to control for differences in the granularity of the prediction bar depending on the invested amount. If for example, $1 was invested, then the 5 monetary values displayed on the prediction bar increased in $0.50 increments, covering a range of $0 and $2 (the min. and max. return). However, if $10 was invested, then the displayed monetary values increased in $5 increments, covering a range of $0 to $20. Because participants were instructed to also consider values between monetary increments on the bar (e.g., between $0 and $5) participants could consider a larger range of plausible returns in the $10 investment scenario. The correspondence between the number of pixels on the screen associated with a particular value was therefore dependent on the investment, potentially leading to reduced precision when indicating predictions in the $10 scenario. To ensure that the dispersion of gazes (i.e., our main readout of uncertainty) did not depend on the pixel resolution of the display bar, we converted all measurements from pixel units to standardized units between 0 and 1 by applying min-max transformation as shown below (Note: x_{min} and x_{max} are the pixel coordinates corresponding to the far left and right edges of the bar, and i indexes each gaze sample).

$$norm\ gaze_i = (raw\ gaze_i - x_{min})/(x_{min} - x_{max})$$

Outcome predictions on trial t were then computed from the mean of range normalized values after transforming them into monetary units:

$$predicted\ outcome_t = \frac{\sum(norm\ gaze_i \times\ investment_t \times\ 2)}{n_{gaze\ samples}}$$

Gaze-based estimate of epistemic uncertainty. Measures of epistemic uncertainty, EU_{gaze}, were simply evaluated as the standard deviation of the min-max normalized gazes on each trial, capturing the predictive precision of one's beliefs about their partner's behavior. Thus, the standard deviation around the mean of participants' gazes allowed us to evaluate whether participants were motivated to precisely track anticipated outcomes from trial to trial, capturing epistemic value information that would not necessarily improve task performance if the choice policy was already optimized. Epistemic uncertainty was calculated from the standard deviation of min-max normalized gazes from each sample, i, for each trial t, where μ_{gaze} is the mean of normalized gaze samples.

$$EU_{gaze_t} = \sqrt{\frac{\sum(norm\ gaze_i - \mu_{gaze_t})^2}{n_{gaze\ samples}}}$$

Gaze-based estimates of policy uncertainty. To compute gaze measures of policy uncertainty—people's tendency to gaze at outcomes that would indicate they are uncertain about what to do—we quantified the proportion of fixations on either side of the outcome boundary using an area-based algorithm. The fixation bar was first divided into hemifields with the outcome boundary serving as the point of separation, such that fixations on the left versus right side of the boundary indicated anticipated monetary losses or gains, respectively. To identify the number of fixations that fell on one or the other side of this boundary, we further divided each hemifield into 50 equidistantly spaced bins, 10 pixels apart. Range-normalized gazes were then placed into respective bins to identify the number fixations on each side of the bar. The proportion of fixations that fell on each side of the outcome boundary, p_{gain} and p_{loss}, were then computed as followed.

$$p_{gain} = \frac{n_{gain\ fixations}}{n_{total\ fixations}}$$

$$p_{loss} = 1 - p_{gain}$$

The proportion of gazes on the gain and loss side of the outcome boundary were use used to calculate gazed-based policy entropy—the empirical analogue to entropy, *H*, calculated from choice probabilities in the Dynamic Bayesian-RL model (Franklin & Frank, 2015; Lamba et al., 2020).

$$H_{gaze_t} = -(p_{gain} \times log_2 p_{gain} - p_{loss} \times log_2 p_{loss})$$

Bayesian Reinforcement Learning models. We tested and compared 4 nested models. The base model, Bayesian Reinforcement Learning (BRL), was identical to the model described in our prior work (Lamba et al., 2020) which readers can reference for additional details. All models use the history of prior outcomes to form Bayesian beliefs about the probability of observing positive or negative outcomes on each trial. Because outcomes in the task resulted in either gains or losses, outcomes can be construed as Bernoulli, and thus $p(\theta)$ as the conjugate—a beta distribution (Daw, 2011).

$$p(\theta|return_{t1} \ldots return_{tn}) = \frac{p(return_{t1} \ldots return_{tn}|\theta) \times p(\theta)}{p(return_{t1} \ldots return_{tn})}$$

Each partner was modeled in a separate distribution and all priors were initialized using the beta distribution conjugate prior (beta 1,1; i.e., uniform). The model assumes that participants are attempting to optimize the policy and hence determine whether it is worth maximally investing (if there is a net gain) or minimally investing (if there is a net loss); this was shown to provide a better fit to the data than a continuous RL model that learns the expected value of each partner (Lamba et al, 2020). Thus, net positive outcomes in the task incremented alpha as +1, and net negative outcomes incremented beta (also as +1). The corresponding mean and variance of the posterior belief (as to whether it is worth investing or not) at the end of each trial can then be calculated as:

$$\mu_{\text{jt}} = \left(\frac{alpha}{alpha + beta}\right) \text{ and } \sigma^2{}_{\text{jt}} = \left(\frac{alpha * beta}{(alpha + beta)^2 * (alpha + beta + 1)}\right)$$

All models used the SoftMax logistic function where ζ and ψ are inverse temperature and bias parameters, respectively. The bias parameter affects the participant-specific threshold for investing the full $10.

$$p(\$1.00) = \frac{e^{\zeta * \mu_{jt}}}{e^{\zeta * \mu_{jt}} + e^{\zeta * \psi}}$$

$$p(\$0.10) = 1 - p(trust\ \$1.00)$$

Note that in a dynamic environment, these Bayesian beliefs become overly narrow (confident) and thus are inflexible to change. To accommodate the belief that the outcomes might change at any time, one can decay the counts of the beta distribution, equivalent to mixing the posterior with a uniform distribution about the partner's value (Daw et al., 2005; Doll et al., 2009). As in our prior work, decay, γ, was modeled separately for gains and losses, allowing for asymmetric decay of past positive or negative experiences. γ_0 indexes baseline beliefs about uncertainty in the task and directly influences how much each observed outcome shapes posterior beliefs. Each γ parameter then adjusts alpha and beta, influencing posterior beliefs such that values closer to 1 allow new evidence to fully update beliefs (i.e., less decay), whereas values closer to 0 increase decay and shrink beliefs back to the prior (i.e., a uniform distribution), effectively forgetting all previously accumulated knowledge.

$$logit(\gamma_{pos}) = \gamma_{0_{pos}}$$
$$logit(\gamma_{neg}) = \gamma_{0_{neg}}$$

$$\alpha_{t+1} = a_t \cdot \gamma_{pos}$$
$$\beta_{t+1} = \beta_t \cdot \gamma_{neg}$$

Dynamic BRL. We tested 3 additional Dynamic BRL models (DBRL), which were identical to BRL except that the decay rate was not fixed. Instead, decay was adjusted from trial to trial as a function of policy uncertainty about whether one should invest the full $10 or not—hence allowing for more flexible updating when more uncertain. Policy uncertainty was modeled as entropy, H, from choice probabilities. When the agent is maximally uncertain about what to do, it assigns equal probability to investing maximally and minimally in the partner, and H =1; when it assigns high probability to either investment, H=0.

$$H_t = -\left[p(\$10.00) \times log_2\left(p(\$10.00)\right) - p(\$1.00) \times log_2\left(p(\$1.00)\right)\right]$$

Changes in entropy from trial to trial, ΔH, additionally influenced decay through γ_1 parameters, such that γ_1 directly amplifies or attenuates the decay rate through changes in policy uncertainty, ΔH.

$$\Delta H = H_t - H_{t-1}$$

$$logit(\gamma_{pos}) = \gamma_{0_{pos}} + \gamma_{1_{pos}} \cdot \Delta H$$
$$logit(\gamma_{neg}) = \gamma_{0_{neg}} + \gamma_{1_{neg}} \cdot \Delta H$$

$$\alpha_{t+1} = a_t \cdot \gamma_{pos}$$
$$\beta_{t+1} = \beta_t \cdot \gamma_{neg}$$

We tested 3 distinct DBRL models that distinguish between the influence of ΔH on posterior beliefs. All models are premised on the normative assumption that increased ΔH signals when one's previous choice policy may no longer be appropriate, and that previously observed outcomes associated with trusting or not trusting should have less impact on future beliefs, effectively reverting beliefs back to a uniform prior distribution. Doing so would allow more recent outcomes to rapidly shape the posterior, which should in principle reflect the statistics of the current environment more accurately. The first model, DBRL-1, was identical to the DBRL model tested in our prior work (Lamba et al, 2020). In this model $\gamma_1$is constrained to negative values so that increasing the negative value of γ_1 amplifies or attenuates the decay rate as a function of ΔH. We tested a second model, DBRL-2, which relaxed the assumption that ΔH only impacts decay by increasing decay rates as ΔH increases. In the DBRL-2 model, γ_1 is a signed parameter, such that positive γ_1 values allow for reduced decay as ΔH increases, thus capturing increased perseveration and faster accumulation of values as ΔH increases. Finally, we tested a threshold model, DBRL-ϕ. Such a model assumes that individuals track trial-to-trial changes in entropy, but only dynamically adjust decay rates when ΔH increases beyond one's threshold value, ϕ (below):

$$logit(\gamma_{pos}) = \gamma_{0_{pos}} + \gamma_{1_{pos}} \cdot (\Delta H - \phi)$$
$$logit(\gamma_{neg}) = \gamma_{0_{neg}} + \gamma_{1_{neg}} \cdot (\Delta H - \phi)$$

Model comparison and validation. Model fits were evaluated using the Akaike information criterion (AIC), which we computed as:

$$AIC = -2(BayesLL) + 2(n\ parameters)$$

We performed model selection using Bayesian Model Selection with the spm_bms function (Stephan et al., 2009) in MATLAB, which we performed separately for high and low anxiety groups. See Supplement for further model validation details.

Acknowledgments. We thank Matthew Nassar for helpful comments and feedback and Eric Ingram for assisting with data collection. **Funding.** This work was funded by the Centers of Biomedical Research Excellence (COBRE), grant no. P20GM103645 awarded to O.F.H. **Author contributions.** A.L., O.F.H, and M.J.F conceptualized the experiment; A.L., collected the data. A.L., did the data analysis under the supervision of O.F.H, and M.J.F; A.L., O.F.H, and M.J.F wrote the manuscript. **Competing interests.** The authors declare no competing interests.

References

Aston-Jones, G., & Cohen, J. D. (2005). An integrative theory of locus coeruleus-norepinephrine function: Adaptive gain and optimal performance. *Annu. Rev. Neurosci.*, *28*, 403–450.

Aylward, J., Valton, V., Ahn, W.-Y., Bond, R. L., Dayan, P., Roiser, J. P., & Robinson, O. J. (2019). Altered learning under uncertainty in unmedicated mood and anxiety disorders. *Nature Human Behaviour*. https://doi.org/10.1038/s41562-019-0628-0

Bakst, L., & McGuire, J. T. (2021). Eye movements reflect adaptive predictions and predictive precision. *Journal of Experimental Psychology: General*, *150*(5), 915.

Bechara, A., Tranel, D., Damasio, H., & Damasio, A. R. (1996). Failure to respond autonomically to anticipated future outcomes following damage to prefrontal cortex. *Cerebral Cortex*, *6*(2), 215–225.

Bennett, D., Niv, Y., & Langdon, A. J. (2021). Value-free reinforcement learning: Policy optimization as a minimal model of operant behavior. *Current Opinion in Behavioral Sciences*, *41*, 114–121.

Berg, J., Dickhaut, J., & McCabe, K. (1995). Trust, reciprocity, and social history. *Games and Economic Behavior*, *10*(1), 122–142.

Bishop, S. J. (2007). Neurocognitive mechanisms of anxiety: An integrative account. *Trends in Cognitive Sciences*, *11*(7), 307–316.

Boelen, P. A., & Reijntjes, A. (2009). Intolerance of uncertainty and social anxiety. *J Anxiety Disord*, *23*(1), 130–135.

Boorman, E. D., O'Doherty, J. P., Adolphs, R., & Rangel, A. (2013). The behavioral and neural mechanisms underlying the tracking of expertise. *Neuron*, *80*(6), 1558–1571.

Browning, M., Behrens, T. E., Jocham, G., O'Reilly, J. X., & Bishop, S. J. (2015). Anxious individuals have difficulty learning the causal statistics of aversive environments. *Nature Neuroscience*, *18*(4), 590–596. https://doi.org/10.1038/nn.3961

Buhr, K., & Dugas, M. J. (2009). The role of fear of anxiety and intolerance of uncertainty in worry: An experimental manipulation. *Behaviour Research and Therapy*, *47*(3), 215–223.

Buss, D. M. (1996). *The evolutionary psychology of human social strategies*.

Carleton, R. N., Mulvogue, M. K., Thibodeau, M. A., McCabe, R. E., Antony, M. M., & Asmundson, G. J. (2012). Increasingly certain about uncertainty: Intolerance of uncertainty across anxiety and depression. *J Anxiety Disord*, *26*(3), 468–479.

Carter, B. T., & Luke, S. G. (2020). Best practices in eye tracking research. *International Journal of Psychophysiology*, *155*, 49–62.

Coddington, L. T., Lindo, S. E., & Dudman, J. T. (2023). Mesolimbic dopamine adapts the rate of learning from action. *Nature*, 1–9.

Cohen, J. D., McClure, S. M., & Yu, A. J. (2007). Should I stay or should I go? How the human brain manages the trade-off between exploitation and exploration. *Philosophical Transactions of the Royal Society B: Biological Sciences*, *362*(1481), 933–942.

Collins, A. G., & Frank, M. J. (2014). Opponent actor learning (OpAL): Modeling interactive effects of striatal dopamine on reinforcement learning and choice incentive. *Psychol Rev*, *121*(3), 337.

Collins, A. G., & Shenhav, A. (2022). Advances in modeling learning and decision-making in neuroscience. *Neuropsychopharmacology*, *47*(1), 104–118.

Cornelissen, F. W., Peters, E. M., & Palmer, J. (2002). The Eyelink Toolbox: Eye tracking with MATLAB and the Psychophysics Toolbox. *Behavior Research Methods, Instruments, & Computers*, *34*(4), 613–617.

Critchley, H. D., Mathias, C. J., & Dolan, R. J. (2001). Neural activity in the human brain relating to uncertainty and arousal during anticipation. *Neuron*, *29*(2), 537–545.

Daw, N. D. (2011). Trial-by-trial data analysis using computational models. *Decision Making, Affect, and Learning: Attention and Performance XXIII*, *23*(1).

Daw, N., Niv, Y., & Dayan, P. (2005). Uncertainty-based competition between prefrontal and dorsolateral striatal systems for behavioral control. *Nature Neuroscience*, *8*(12), 1704–1711. https://doi.org/10.1038/nn1560

Diaconescu, A. O., Mathys, C., Weber, L. A., Daunizeau, J., Kasper, L., Lomakina, E. I., Fehr, E., & Stephan, K. E. (2014). Inferring on the intentions of others by hierarchical Bayesian learning. *PLoS Computational Biology*, *10*(9), e1003810. https://doi.org/10.1371/journal.pcbi.1003810

Doll, B. B., Jacobs, W. J., Sanfey, A. G., & Frank, M. J. (2009). Instructional control of reinforcement learning: A behavioral and neurocomputational investigation. *Brain Res*, *1299*, 74–94. https://doi.org/10.1016/j.brainres.2009.07.007

Fehr, E., Fischbacher, U., & Kosfeld, M. (2005). Neuroeconomic foundations of trust and social preferences: Initial evidence. *American Economic Review*, *95*(2), 346–351.

FeldmanHall, O., Glimcher, P., Baker, A. L., & Phelps, E. A. (2016). Emotion and decision-making under uncertainty: Physiological arousal predicts increased gambling during ambiguity but not risk. *Journal of Experimental Psychology: General*, *145*(10), 1255.

FeldmanHall, O., & Nassar, M. R. (2021). The computational challenge of social learning. *Trends in Cognitive Sciences*, *25*(12), 1045–1057.

FeldmanHall, O., & Shenhav, A. (2019). Resolving uncertainty in a social world. *Nature Human Behaviour*, *3*(5), 426–435.

Frank, M. J., & Claus, E. D. (2006). Anatomy of a decision: Striato-orbitofrontal interactions in reinforcement learning, decision making, and reversal. *Psychol Rev*, *113*(2), 300.

Franklin, N. T., & Frank, M. J. (2015). A cholinergic feedback circuit to regulate striatal population uncertainty and optimize reinforcement learning. *Elife*, *4*. https://doi.org/10.7554/eLife.12029

Friston, K. J., Lin, M., Frith, C. D., Pezzulo, G., Hobson, J. A., & Ondobaka, S. (2017). Active inference, curiosity and insight. *Neural Computation*, *29*(10), 2633–2683.

Gagne, C., Zika, O., Dayan, P., & Bishop, S. J. (2020). Impaired adaptation of learning to contingency volatility in internalizing psychopathology. *Elife*, *9*, e61387.

Garland, R. (1991). The mid-point on a rating scale: Is it desirable. *Marketing Bulletin*, *2*(1), 66–70.

Gottlieb, J., Hayhoe, M., Hikosaka, O., & Rangel, A. (2014). Attention, reward, and information seeking. *Journal of Neuroscience*, *34*(46), 15497–15504.

Gottlieb, J., & Oudeyer, P.-Y. (2018). Towards a neuroscience of active sampling and curiosity. *Nature Reviews Neuroscience*, *19*(12), 758–770.

Gottlieb, J., Oudeyer, P.-Y., Lopes, M., & Baranes, A. (2013). Information-seeking, curiosity, and attention: Computational and neural mechanisms. *Trends in Cognitive Sciences*, *17*(11), 585–593.

Hare, T. A., O'doherty, J., Camerer, C. F., Schultz, W., & Rangel, A. (2008). Dissociating the role of the orbitofrontal cortex and the striatum in the computation of goal values and prediction errors. *Journal of Neuroscience*, *28*(22), 5623–5630.

Harris, D., Vine, S., Wilson, M., & Arthur, T. (2023). *The relationship between environmental statistics and predictive gaze behaviour during a manual interception task: Eye movements as active inference*.

Holmqvist, K., Nyström, M., & Mulvey, F. (2012). *Eye tracker data quality: What it is and how to measure it*. 45–52.

Ishii-Kuntz, M. (1990). Social interaction and psychological well-being: Comparison across stages of adulthood. *The International Journal of Aging and Human Development*, *30*(1), 15–36.

Jaskir, A., & Frank, M. J. (2023). On the normative advantages of dopamine and striatal opponency for learning and choice. *Elife*, *12*, e85107.

Koerner, N., & Dugas, M. J. (2006). A cognitive model of generalized anxiety disorder: The role of intolerance of uncertainty. *Worry and Its Psychological Disorders: Theory, Assessment and Treatment*, 201–216.

Kramer, R. M., & Wei, J. (2014). Social uncertainty and the problem of trust in social groups: The social self in doubt. In *The psychology of the social self* (pp. 145–168). Psychology Press.

Lamba, A., Frank, M. J., & FeldmanHall, O. (2020). Anxiety impedes adaptive social learning under uncertainty. *Psychological Science*, *31*(5), 592–603.

Leckey, S., Selmeczy, D., Kazemi, A., Johnson, E. G., Hembacher, E., & Ghetti, S. (2020). Response latencies and eye gaze provide insight on how toddlers gather evidence under uncertainty. *Nature Human Behaviour*, *4*(9), 928–936.

Li, J., & Daw, N. D. (2011). Signals in human striatum are appropriate for policy update rather than value prediction. *Journal of Neuroscience*, *31*(14), 5504–5511.

Li, J., Schiller, D., Schoenbaum, G., Phelps, E. A., & Daw, N. D. (2011). Differential roles of human striatum and amygdala in associative learning. *Nature Neuroscience*, *14*(10), 1250–1252.

Littman, M. L. (1994). *Memoryless policies: Theoretical limitations and practical results*. *3*, 238.

Löwe, B., Decker, O., Muller, S., Brahler, E., Schellberg, D., Herzog, W., & Herzberg, P. Y. (2008). Validation and standardization of the Generalized Anxiety Disorder Screener (GAD-7) in the general population. *Med Care*, *46*(3), 266–274. https://doi.org/10.1097/MLR.0b013e318160d093

Mathys, C. D., Lomakina, E. I., Daunizeau, J., Iglesias, S., Brodersen, K. H., Friston, K. J., & Stephan, K. E. (2014). Uncertainty in perception and the Hierarchical Gaussian Filter. *Front Hum Neurosci*, *8*, 825.

Mnih, V., Kavukcuoglu, K., Silver, D., Rusu, A. A., Veness, J., Bellemare, M. G., Graves, A., Riedmiller, M., Fidjeland, A. K., & Ostrovski, G. (2015). Human-level control through deep reinforcement learning. *Nature*, *518*(7540), 529–533.

Nachum, O., Norouzi, M., Xu, K., & Schuurmans, D. (2017). Bridging the gap between value and policy based reinforcement learning. *Advances in Neural Information Processing Systems*, *30*.

Nassar, M. R., Bruckner, R., & Frank, M. J. (2019). Statistical context dictates the relationship between feedback-related EEG signals and learning. *Elife*, *8*, e46975.

Nassar, M. R., Rumsey, K. M., Wilson, R. C., Parikh, K., Heasly, B., & Gold, J. I. (2012). Rational regulation of learning dynamics by pupil-linked arousal systems. *Nature Neuroscience*, *15*(7), 1040–1046. https://doi.org/10.1038/nn.3130

Nassar, M. R., Wilson, R. C., Heasly, B., & Gold, J. I. (2010). An approximately Bayesian delta-rule model explains the dynamics of belief updating in a changing environment. *J Neurosci*, *30*(37), 12366–12378. https://doi.org/10.1523/jneurosci.0822-10.2010

Niv, Y., Daw, N. D., & Dayan, P. (2006). Choice values. *Nature Neuroscience*, *9*(8), 987–988.

Niv, Y., & Langdon, A. (2016). Reinforcement learning with Marr. *Current Opinion in Behavioral Sciences*, *11*, 67–73.

Palminteri, S., Khamassi, M., Joffily, M., & Coricelli, G. (2015). Contextual modulation of value signals in reward and punishment learning. *Nature Communications*, *6*(1), 8096.

Parr, T., & Friston, K. J. (2017). Uncertainty, epistemics and active inference. *Journal of the Royal Society Interface*, *14*(136), 20170376.

Payzan-LeNestour, E., & Bossaerts, P. (2011). Risk, unexpected uncertainty, and estimation uncertainty: Bayesian learning in unstable settings. *PLoS Computational Biology*, *7*(1), e1001048.

Rajkowski, J. (1993). Correlations between locus coeruleus (LC) neural activity, pupil diameter and behavior in monkey support a role of LC in attention. *Soc. Neurosc., Abstract, Washington, DC, 1993*.

Rushworth, M. F., & Behrens, T. E. (2008). Choice, uncertainty and value in prefrontal and cingulate cortex. *Nature Neuroscience*, *11*(4), 389–397.

Salvucci, D. D., & Goldberg, J. H. (2000). *Identifying fixations and saccades in eye-tracking protocols*. 71–78.

Schulz, E., & Gershman, S. J. (2019). The algorithmic architecture of exploration in the human brain. *Curr Opin Neurobiol*, *55*, 7–14.

Siegel, J. Z., Mathys, C., Rutledge, R. B., & Crockett, M. J. (2018). *Beliefs about bad people are volatile*. *2*(10), 750–756. https://doi.org/10.1038/s41562-018-0425-1

Siegle, G. J., Ichikawa, N., & Steinhauer, S. (2008). Blink before and after you think: Blinks occur prior to and following cognitive load indexed by pupillary responses. *Psychophysiology*, *45*(5), 679–687.

Spielberger, C. D. (1983). *State-trait anxiety inventory for adults*.

Spitzer, R. L., Kroenke, K., Williams, J. B. W., & Löwe, B. (2006). A Brief Measure for Assessing Generalized Anxiety Disorder: The GAD-7. *Archives of Internal Medicine*, *166*(10), 1092–1097. https://doi.org/10.1001/archinte.166.10.1092

Stephan, K. E., Penny, W. D., Daunizeau, J., Moran, R. J., & Friston, K. J. (2009). Bayesian model selection for group studies. *Neuroimage*, *46*(4), 1004–1017.

Subedi, B. P. (2016). Using Likert type data in social science research: Confusion, issues and challenges. *International Journal of Contemporary Applied Sciences*, *3*(2), 36–49.

Sutton, R. S., & Barto, A. G. (2018). *Reinforcement learning: An introduction*. MIT press.

Tomov, M. S., Truong, V. Q., Hundia, R. A., & Gershman, S. J. (2020). Dissociable neural correlates of uncertainty underlie different exploration strategies. *Nature Communications*, *11*(1), 2371.

Urai, A. E., Braun, A., & Donner, T. H. (2017). Pupil-linked arousal is driven by decision uncertainty and alters serial choice bias. *Nature Communications*, *8*(1), 14637.

Vives, M.-L., & FeldmanHall, O. (2018). Tolerance to ambiguous uncertainty predicts prosocial behavior. *Nature Communications*, *9*(1), 1–9.

Wilson, R. C., Bonawitz, E., Costa, V. D., & Ebitz, R. B. (2021). Balancing exploration and exploitation with information and randomization. *Current Opinion in Behavioral Sciences*, *38*, 49–56.

Wilson, R. C., Geana, A., White, J. M., Ludvig, E. A., & Cohen, J. D. (2014). Humans use directed and random exploration to solve the explore–exploit dilemma. *Journal of Experimental Psychology: General*, *143*(6), 2074.

Wittek, P., Liu, Y.-H., Darányi, S., Gedeon, T., & Lim, I. S. (2016). Risk and ambiguity in information seeking: Eye gaze patterns reveal contextual behavior in dealing with uncertainty. *Frontiers in Psychology*, *7*, 1790.

Yu, A. J., & Dayan, P. (2005). Uncertainty, neuromodulation, and attention. *Neuron*, *46*(4), 681–692. https://doi.org/10.1016/j.neuron.2005.04.026

SUPPLEMENT

Keeping an eye out for change: Anxiety disrupts adaptive resolution of policy and epistemic uncertainty

Amrita Lamba, Michael J. Frank, Oriel FeldmanHall

Supplementary Data Analysis

Validation of gaze-based uncertainty measures. To ensure that gaze-based predictions were reliably tracking estimates of each partner's behavior, we evaluated whether the mean location of fixations on the prediction bar corresponded with actual monetary returns. A mixed-effects regression revealed that gaze location during the prediction phase significantly predicted the percentage of the investment returned during the feedback phase (t = 33.87, p < .001; Fig. S1A), demonstrating that gaze-derived trial predictions were reliably rooted in forthcoming monetary outcomes. Participants also expressed greater policy uncertainty when they were unsure of the optimal choice policy in the task (t = -6.77, p < .001; Fig. S1B). However, once participants knew the optimal policy, they expressed greater epistemic uncertainty (t = 10.26, p < .001), suggesting that periods of optimized behavior were accompanied by a desire to learn more about partners. H_{gaze} was also greatest on trials where the partner's behavior was ambiguous and not associated with a clear choice policy, compared to when partners were either maximally trustworthy or untrustworthy (t = 3.965, p < .001; Fig. S1C), suggesting that H_{gaze} captures the relative difficulty of learning the optimal choice rule in the task.

Entropy and choice variability. Based on our prior work (Lamba et al., 2020), policy uncertainty can be behaviorally indexed as increased choice variability—indeed higher choice entropy, *H,* should imply more wavering between choice options, which also serves to modulate learning in changing environments (Franklin & Frank, 2015). In contrast, reduced choice variability could index anchoring onto prior learning rules which is effective in a stable environment, but leads to slower adaptation in volatile conditions. Notably, the link between behaviorally expressed choice conflict and physiological expressions of policy uncertainty has never been tested, and thus it remains unclear whether individuals who express policy uncertainty at the physiological level indeed behaviorally manifest this uncertainty as increased choice conflict. We thus assessed whether choice variability was related to physiologically expressed policy uncertainty (H_{gaze}), and whether this relationship differed with anxiety.

To quantify choice variability, we calculated the standard deviation of participant investments per task block (i.e., every 4 trials) for each partner type, resulting in approximately 24 choice variability measurements per participant. A linear mixed-effects model revealed a significant interaction between policy uncertainty and anxiety on choice variability (t = -3.140, p = .0017; Fig. S2), in which greater expression of H_{gaze} were associated with increased choice variability in the low anxiety group, but reduced choice variability in the high anxiety group. Further, this effect was heightened in the loss domain; the interaction effect between policy uncertainty, anxiety level, and outcome valence was marginally significant (t = 1.95, p =.0517). These findings indicate

that H_{gaze} increases choice variability in the low anxiety group in line with normative models (Franklin & Frank, 2015), whereas H_{gaze} is associated with increased choice perseveration in people with high anxiety.

Model Comparison and Validation

Bayesian Reinforcement Learning models and parameters. We tested and compared a set of 4 nested Bayesian Reinforcement Learning (BRL) models, 3 of which included additional γ_1 terms to dynamically adjust the decay rate (DBRL). The set of models considered, and their corresponding free parameters, are shown in Table S1. Table S2 and Fig. S3 show the mean performance of each model, indexed as the mean negative AIC. Mean AIC values show that the DBRL-2 model best captures choice data in the task, which was additionally supported with Bayesian model selection. Descriptions of each free parameter in the DBRL-2 model are provided in Table S3. Parameters were optimized individually for each participant using the fmincon gradient descent function in MATLAB with 20 iterations (i.e., starting points) per model.

Model validation. We performed MLE and parameter recovery checks to ensure that the winning model, DBRL-2, adequately captured participant behavior in the task and parameter fits were reliable. To ensure that the MLE-optimized parameters could reproduce behavior in the task, we simulated choices from the optimized set of parameters for each participant. As shown in Fig. 4A, the DBRL-2 model captures overall choice profiles in both high and low anxiety groups, and in particular, the slowed learning patterns in the high anxiety group. We assessed parameter recovery by fitting simulated data to the model and comparing the corresponding recovered parameters to the original set of MLE-optimized parameters evaluated from each participant's choice data. Parameter recovery tests shown in Fig. S4 show that DBRL-2 parameters are reliable.

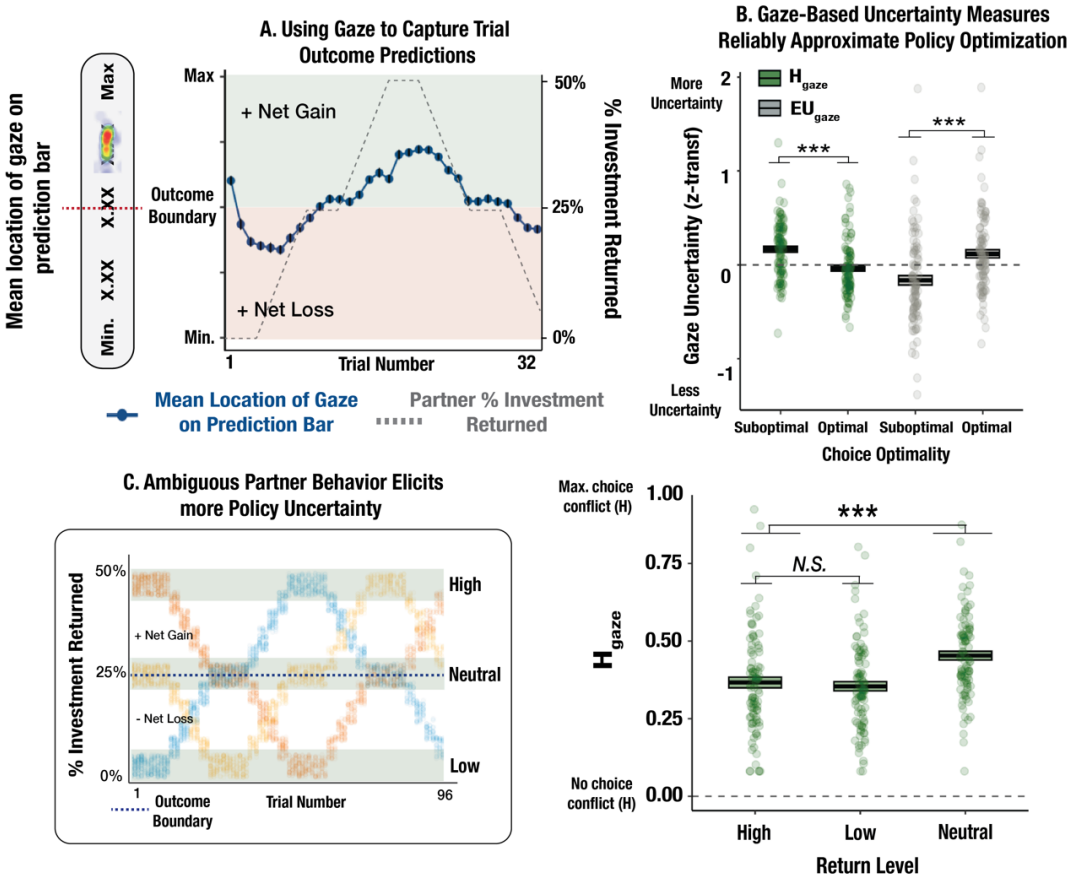

Figure S1. Variability in gaze patterns reflects anticipated monetary outcomes and knowledge about the optimal choice policy. A. *Using gaze to capture trial outcome predictions. Panel shows correspondence between gaze-based predictions and trial outcomes for an example partner type. Across all partner types, gaze fixations on the bar during the prediction phase tracked the percentage of the investment returned during the feedback phase, validating the use of gaze-based measures to assess beliefs about task outcomes.* ***B.*** *Gaze-based uncertainty measures reliably approximate policy optimization. Participants indicated greater policy uncertainty on trials in which the suboptimal response was selected and greater epistemic uncertainty on trials in which the optimal response was selected, demonstrating that uncertainty estimates from gaze patterns capture knowledge about the optimal choice policy. Individual points correspond to mean participant estimates of each uncertainty type. Box width shows the standard error of the mean.* ***C.*** *Ambiguous partner behavior elicits more policy uncertainty. Participants expressed greater policy uncertainty on neutral trials in which there was no discernable payoff-maximizing response, compared to high and low return trials in which the optimal choice was unambiguous. Asterisks (*,**,***) denote p < .05, p < .01, p < .001, respectively. Errors bars indicate the standard error of the mean.*

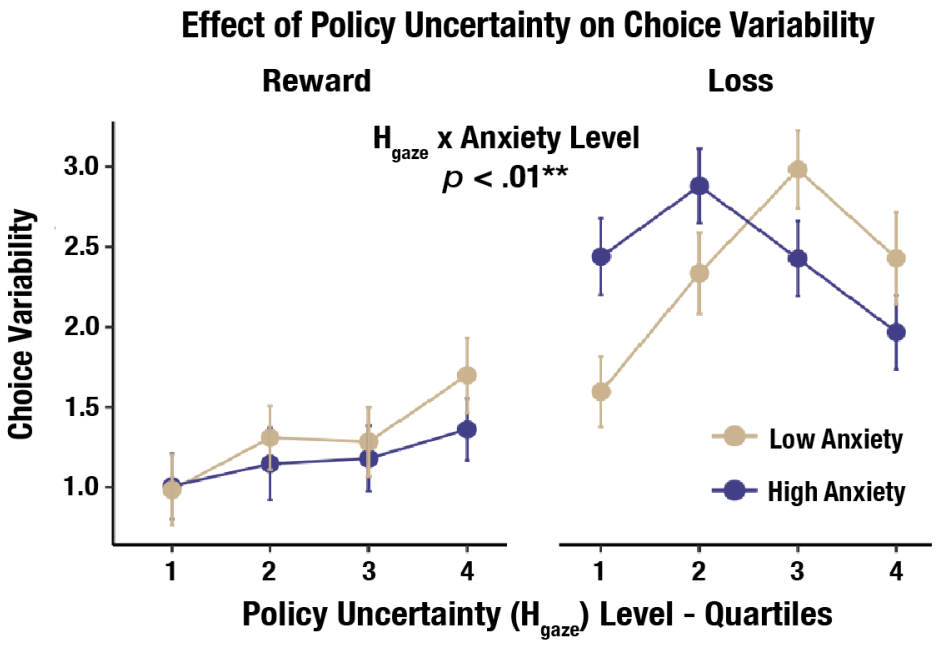

Figure S2. Effect of policy uncertainty on choice variability. *In the low anxiety group, choice variability increases with gaze-measures of policy uncertainty, in line with the presumed effect of increased policy uncertainty on choice conflict. In contrast, policy uncertainty is associated with reduced choice variability in the high anxiety group, particularly on loss trials in which anxious participants tend to overinvest in untrustworthy partners. For visualization, data from each trial was binned into policy uncertainty quartiles along the x-axis. Statistics were conducted using the raw, un-binned policy uncertainty measures.*

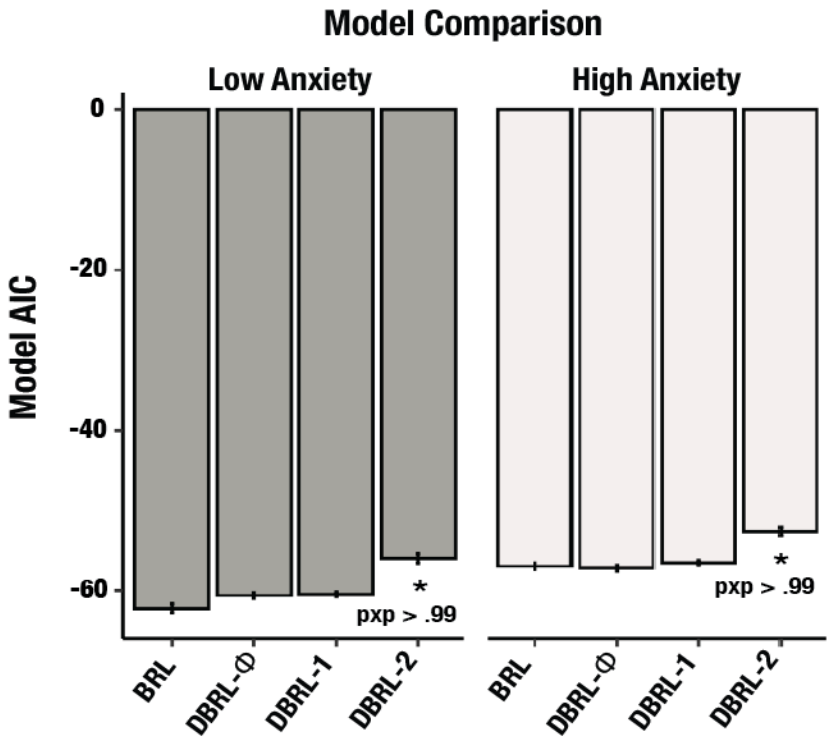

Figure S3. Model comparison*. Across both high and low anxiety groups, the DBRL-2 model best captured choice behavior in the task, indicated by the max. negative AIC. *pxp denotes the protected exceedance probability for the winning model from Bayesian Model Selection.*

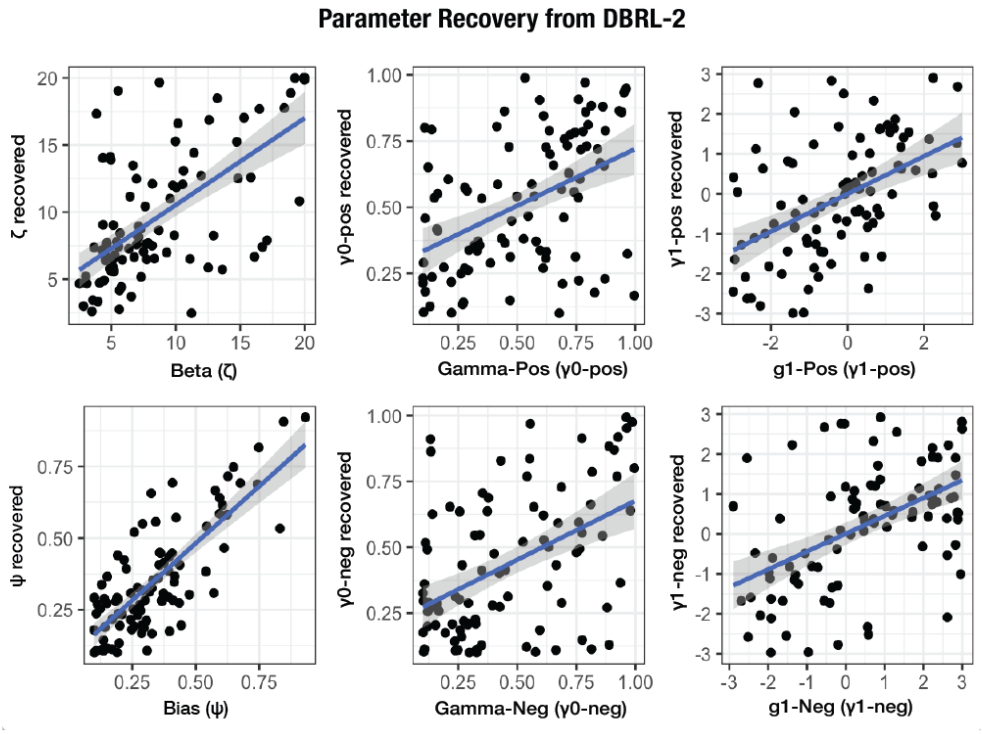

Figure S4. Parameter recovery. *The reliability of all free parameters in the DBRL-2 model was evaluated by comparing the set of MLE-optimized parameters from choice data (x-axis) to the set of parameters evaluated from simulated data (y-axis). All parameters were generally recoverable, indicating that the DBRL-2 model provides reliable fits.*

Model No.	***Model***	ζ	ψ	$\gamma_{0_{pos}}$	$\gamma_{0_{neg}}$	$\gamma_{1_{pos}}$	$\gamma_{1_{neg}}$	ϕ	***No. params***
1	BRL	×	×	×	×				4
2	DBRL-1	×	×	×	×	×	×		6
3	DBRL-2	×	×	×	×	×	×		6
4	DBRL-ϕ	×	×	×	×	×	×	×	7

Table S1. *List of BRL models included in model comparison, including their respective free parameters indicated with the ×. See methods for a brief description of each model. Descriptions of each parameter are included in Table S3.*

Model No	***Model***	***Anxiety Group***	***Mean AIC***	***SE***
1	BRL	Low	-62.23	0.60
		High	-56.98	0.41
2	DBRL-1	Low	-60.49	0.31
		High	-56.55	0.30
3	DBRL-2	Low	-56.03*	0.57
		High	-52.65*	0.51
4	DBRL-ϕ	Low	-60.64	0.37
		High	-57.22	0.39

Table S2. *Mean AIC and SE for each model across high and low anxiety groups. *Denotes the best-fitting model in the set, indexed as the max. negative AIC.*

Model Parameter	*Parameter Description*	*Upper-bound*	*Lower-bound*
Inverse Temperature ζ	Degree to which participant exploits learned decision-rule associated with rewarding outcomes through deterministic vs. exploratory behavior	20 - highly deterministic behavior	1 - always selects at random
Bias ψ	Benchmark for investing (i.e. how much additional value does the participant need to derive from investing $10 in order to select the choice over a preferred strategy to always invest $1)	1.0 - high benchmark for investing (participant is biased towards never investing $10)	0.1 – low benchmark for investing (participant is biased towards always investing $10)
Negative Decay Intercept $\gamma_{0_{neg}}$	Degree of decay of negative outcomes, which prevents the posterior distribution from becoming overly confident (certain) from previous experience	1.0 – no decay (posterior distribution is updated from negative outcomes and previous experiences accumulate)	0.1 – maximal decay (added uncertainty prevents posterior distribution from integrating observed negative outcomes over experience)
Positive Decay Intercept $\gamma_{0_{pos}}$	Degree of decay or uncertainty over positive outcomes	1.0– no decay (posterior distribution is updated from positive outcomes and previous experiences accumulate)	0.1 – maximal decay (added uncertainty prevents posterior distribution from integrating observed positive outcomes)
Negative Dynamic Decay $\gamma_{1_{neg}}$	Extent to which negative outcomes are decayed as a function of change points in uncertainty	2 – Faster accumulation of values as a function of ΔH	-2.0—maximal adjustment of decay rate as a function of ΔH
Positive Dynamic Decay $\gamma_{1_{pos}}$	Extent to which positive outcomes are decayed as a function of change points in uncertainty	2 – Faster accumulation of values as a function of ΔH	-2.0—maximal adjustment of decay rate as a function of ΔH

Table S3. *Description of DBRL-2 model parameters. Note, model parameters are identical to the original model developed in our prior work (Lamba et al., 2020), with the exception of the upper bounds of the* γ_1 *parameters.* γ_1 *was constrained to negative values in our original model such that greater entropy could only modulate the decay rate by linearly increasing or deceasing decay as a function of* ΔH*. This constraint was relaxed in DBRL-2, allowing for the opposite pattern in which* ΔH *speeds accumulation of values as entropy increases (positive* γ_1 *values).*

References

Franklin, N. T., & Frank, M. J. (2015). A cholinergic feedback circuit to regulate striatal population uncertainty and optimize reinforcement learning. *Elife*, *4*. https://doi.org/10.7554/eLife.12029

Lamba, A., Frank, M. J., & FeldmanHall, O. (2020). Anxiety impedes adaptive social learning under uncertainty. *Psychological Science*, *31*(5), 592–603.